**SpezialForschungsBereich F 32**

Karl–Franzens Universität Graz
Technische Universität Graz
Medizinische Universität Graz

# Functional-Analytic and Numerical Issues in Splitting Methods for Total Variation-based Image Reconstruction

M. Hintermüller C. N. Rautenberg J. Hahn

SFB-Report No. 2013-008 July 2013

A–8010 GRAZ, HEINRICHSTRASSE 36, AUSTRIA

Supported by the
Austrian Science Fund (FWF)

SFB sponsors:

- **Austrian Science Fund** (FWF)
- **University of Graz**
- **Graz University of Technology**
- **Medical University of Graz**
- **Government of Styria**
- **City of Graz**

# FUNCTIONAL-ANALYTIC AND NUMERICAL ISSUES IN SPLITTING METHODS FOR TOTAL VARIATION-BASED IMAGE RECONSTRUCTION *

MICHAEL HINTERMÜLLER†, CARLOS N. RAUTENBERG‡, AND JOOYOUNG HAHN §

**Abstract.** Variable splitting schemes for the function space TV-model in its primal and pre-dual formulations are considered. In the primal splitting formulation, while existence of a solution cannot be guaranteed, it is shown that quasi-minimizers of the penalized problem are asymptotically related to the solution of the original TV-model. On the other hand, for the pre-dual formulation a family of parametrized problems is introduced and a parameter dependent contraction of an associated fixed point iteration is established. Moreover, the theory is validated by numerical tests. Additionally, the augmented Lagrangian approach is studied, details on an implementation on a staggered grid are provided and numerical tests are shown.

**Key words.** Augmented Lagrangian, Bregman iteration, image reconstruction, penalty method, splitting methods, total variation regularization.

**AMS subject classifications.** 94A08, 49M29, 65K05

## 1. Introduction.

Variable splitting and associated alternating algorithms have been recently successfully applied to discrete models in image reconstruction and denoising based on total variation (TV) regularization; see for example, [7, 9, 20, 26–28]. The basic idea consists in the introduction of one or more new variables, a penalized problem and the resolution of two (or more) minimization problems significantly simpler than the original one. Algorithmically, this results in a sequence of nested iterations, which, on the discrete level, may exhibit an (image) resolution dependent convergence. As the penalty parameter is increased, one nevertheless expects that the solution of the original problem is approached. While this expectation may be justified in finite dimensions, in infinite dimensions new difficulties arise which render the existence of solutions of various sub-problems and the passage to the limit with the pertinent penalty parameter as delicate matters.

To the best of our knowledge, infinite dimensional analysis of such splitting and alternating minimization approaches in the appropriate Banach space setting have not yet been considered in the context of the TV-model. Typically, rather the finite dimensional problem is studied in the literature. The work by Setzer in [22] comes closest to the aforementioned function space analysis. However, it is confined to problems in Hilbert space settings only, whereas the TV-model requires the non-reflexive space of functions of bounded variations as the associated solution space.

*This work was supported by the Austrian Ministry of Science and Education and the Austrian Science Fund FWF through START-Project Y305 Interfaces and Free Boundaries, and the SFB Project F32 04-N18 "Mathematical Optimization and Its Applications in Biomedical Sciences," the German Research Foundation DFG Research Center MATHEON through Projects C28, and the DFG Priority Program SPP 1253 through project Elliptic Mathematical Programs with Equilibrium Constraints (MPECs) in Function Space: Optimality Conditions and Numerical Realization.

†Department of Mathematics, Humboldt-University of Berlin, Unter den Linden 6, 10099 Berlin, Germany. (hint@math.hu-berlin.de).

‡Department of Mathematics and Scientific Computing, Karl-Franzens-University of Graz, Heinrichstrasse 36, A-8010 Graz, Austria. (carlos.rautenberg@uni-graz.at)

§The research for this work was performed while J.H. was a member of the SFB F32 04-N18 "Mathematical Optimization and Its Applications in Biomedical Sciences" at the Karl-Franzens-University of Graz. Current affiliation: AVL, Alte Poststrasse 152, 8010, Graz, Austria. (jooyounghahn@gmail.com)

In the present paper, we are interested in studying splitting and associated alternating direction methods in function space; more precisely in the original non-reflexive Banach space associated with the TV-model. In this context we consider the primal as well as the pre-dual formulations of the problem, and we study associated splitting techniques. Interestingly, it turns out that the existence of a solution to the associated penalized primal problem cannot be guaranteed, in general. Rather $\epsilon$-minimizers in the sense of Ekeland's variational principle can be assured only. For the penalized pre-dual problem, however, solutions do exist. As a consequence, the Bregman iteration or augmented Lagrangian schemes are not well defined in the primal context but can be shown to converge when applied to solving the pre-dual problem. We emphasize that, upon discretization, such distinct features get lost.

The pre-dual problem is posed in the Hilbert space $H_0(\mathrm{div})$, which is the space of $\mathbf{L}^2$-vector fields whose divergence is an element of $L^2(\Omega)$ as well. For this reason we suggest a discretization of the penalized (and associated) pre-dual problem on staggered grids. It is shown that this approach compares favorably to energy based discretization techniques such as the one in [6].

In order to understand the difficulties associated when moving from finite dimensional into infinite dimensional spaces, it is useful to consider the following. In finite dimensions, the primal formulation of the TV-model without blurring reads:

$$\min \sum_i \frac{1}{2}|u_i - f_i|^2 + \alpha|(\nabla_h u)_i|_{\ell^2} \quad \text{over } u \in \mathbb{R}^{n\times n}, \tag{1.1}$$

where $\nabla_h$ is a discrete gradient, $|\cdot|_{\ell^2}$ is the $\ell^2$-norm in $\mathbb{R}^2$, $\alpha > 0$ is the regularization parameter, and $f \in \mathbb{R}^{n\times n}$ is a given (possibly noisy) image. In this problem, for the application of the an alternating minimization scheme, a new variable $\mathbf{p} = (p_1, p_2)$, with $p_1, p_2 \in \mathbb{R}^{n\times n}$, is introduced and the following penalized version is considered:

$$\min \sum_i \frac{1}{2}|u_i - f_i|^2 + \alpha|\mathbf{p}_i|_{\ell^2} + \frac{r}{2}|(\nabla_h u)_i - \mathbf{p}_i|^2_{\ell^2} \quad \text{over } u \in \mathbb{R}^{n\times n},\ \mathbf{p} \in \mathbb{R}^{n\times n} \times \mathbb{R}^{n\times n}, \tag{1.2}$$

where $r > 0$ denotes the penalty parameter. For large $r > 0$, it can be shown that this problem is related to (1.1). On the other hand, the infinite dimensional analogue to the TV-model is

$$\min \frac{1}{2}\int_\Omega |u - f|^2 + \alpha|\mathcal{D}u|(\Omega) \quad \text{over } u \in BV(\Omega), \tag{1.3}$$

where $|\mathcal{D}u|(\Omega)$ is the total mass of the Borel measure $\mathcal{D}u$ determined by the distributional derivative of $u$, and $f \in L^2(\Omega)$. If we follow the same procedure as in the finite dimensional case, we need to introduce a new variable $\mathbf{p}$ in the same space as $\mathcal{D}u$, that is, $\mathbf{p}$ should be a Borel measure. As a consequence, the penalty term $\frac{r}{2}|\mathcal{D}u - \mathbf{p}|^2_{L^2}$ appears no longer appropriate, since $\mathbf{p}$ nor $\mathcal{D}u$ need to belong to $L^2(\Omega)$ and might have no pointwise description over $\Omega$. Ignoring this fact and nevertheless adding $\frac{r}{2}|\mathcal{D}u - \mathbf{p}|^2_{L^2}$ to the objective in (1.3) with $|\mathcal{D}u|(\Omega)$ replaced by $|\mathbf{p}|_{\mathbf{L}^1}$ significantly changes the nature of the problem. As a consequence, existence of a solution $(u_r^*, \mathbf{p}_r^*)$ to the resulting penalty problem cannot be guaranteed, in general. Furthermore, in case the penalty term is taken to be $\frac{r}{2}|\mathcal{D}u - \mathbf{p}|(\Omega)$, then, although the problem is now well-defined as we prove in section 2.1, there are no advantages in the splitting approach over the original TV-formulation. This discussion is continued in Section 2.1 below where a solution to this issue is also proposed. In the case of the pre-dual formulation, similar (yet simpler) challenges are faced and solved in Section 3.1.

In section 2 we are concerned with a variable splitting approach for the primal formulation of the TV-model. We provide an infinite dimensional penalty framework based on $\epsilon$-minimizers in a sufficient regular state space which is amenable to numerical implementation. Under appropriate conditions it is proven that the sequence of $\epsilon$-minimizers converges to the solution of (1.3). Furthermore, provided regularity and boundedness assumptions hold true, we show that an augmented Lagrangian-looking penalty functional exhibits the same behavior than the pure penalty method.

Section 3 is devoted to the variable splitting approach for the Fenchel pre-dual formulation of the TV-model. It is proven (Lemma 3.1) that the sequence of minimizers of the associated penalized problem is well-defined and converges (in a certain sense) to the solution of the pre-dual problem. It is also shown that an augmented Lagrangian approach is suitable for the infinite dimensional problem, in the sense that there exists a Lagrange multiplier such that the solution of the splitting problem for the pre-dual formulation is a global minimizer of the augmented Lagrangian, without the necessity of a limiting process for the penalty parameter.

Details of a numerical implementation on a staggered grid for the pre-dual formulation are provided in Section 4. We also show compatibility properties of the discrete divergence and gradient operators. The section ends with comparative results obtained by the algorithms specified in the paper and in the existing literature.

**Notation.** Let $\Omega \subset \mathbb{R}^2$ be a bounded and open domain. We denote by $L^p(\Omega)$ the usual Lebesgue space of real-valued functions on the domain $\Omega$. The space $\mathbf{L}^p(\Omega)$ is defined as $L^p(\Omega) \times L^p(\Omega)$ such that $\mathbf{f} := (f_1, f_2) : \Omega \to \mathbb{R}^2$ belongs to $\mathbf{L}^p(\Omega)$ iff $f_i \in L^p(\Omega)$ for $i = 1, 2$. The Sobolev space $W^{1,1}(\Omega)$ contains weakly differentiable functions in $L^1(\Omega)$ whose weak derivatives also belong to $\mathbf{L}^1(\Omega)$ (see [1] for a definition of the Sobolev space). It is endowed with the norm $|v|_{W^{1,1}} = |v|_{L^1} + |\nabla v|_{\mathbf{L}^1}$. Throughout the paper, strong convergence is denoted by "$\to$" and weak convergence by "$\rightharpoonup$". For a vector $\mathbf{x} \in \mathbb{R}^2$, the Euclidian norm is denoted either by $|\mathbf{x}|_{\ell^2}$ or $|\mathbf{x}|$.

The Lebesgue measure of a measurable set $\Omega$ is denoted as $|\Omega|$, and we say that a property holds "a.e. in $\Omega$", if it is true in $\Omega$ except for a subset $\Omega_0 \subset \Omega$ such that $|\Omega_0| = 0$.

We denote by $\mathscr{L}(V, W)$ the vector space of linear bounded operators between the normed vector spaces $V$ and $W$ with norm $|G|_{\mathscr{L}(V,W)} = \sup_{|v|_V=1} |Gv|_W$, for $G \in \mathscr{L}(V, W)$.

The following results can be found on [3], which we also follow closely notationwise. We denote the set of $\mathbb{R}^2$-valued Borel measures by $\mathbf{M}(\Omega; \mathbb{R}^2)$. If $B$ is a Borel set, then then total mass $|\mu|(B)$ for $\mu \in \mathbf{M}(\Omega; \mathbb{R}^2)$ is defined as

$$|\mu|(B) = \sup \left\{ \sum_{i=0}^{\infty} |\mu(B_i)| : \quad \bigcup_{i=0}^{\infty} B_i = B \right\}, \tag{1.4}$$

where the supremum is taken over all partitions of $B$ in its Borel field. Note that $\mathbf{M}(\Omega; \mathbb{R}^2)$ is a Banach space when endowed with the norm $\mu \mapsto |\mu|(\Omega)$. Additionally, if $\mu \in \mathbf{M}(\Omega; \mathbb{R}^2)$, then $|\mu|$ is a non-negative Borel measure and $|\mu|(B) = \int_B \mathrm{d}|\mu|$.

The space of functions of bounded variation over $\Omega$ is denoted as $BV(\Omega)$ and it is defined to be the space of functions $u \in L^1(\Omega)$ with gradient $\mathcal{D}u$ (in the distributional sense) in $\mathbf{M}(\Omega; \mathbb{R}^2)$. Endowed with the norm

$$|u|_{BV} = |u|_{L^1} + |\mathcal{D}u|(\Omega),$$

$BV(\Omega)$ becomes a Banach space, and we write $\int_\Omega |\mathcal{D}u| := |\mathcal{D}u|(\Omega)$ (in order to avoid the notation $\int_\Omega \mathrm{d}|\mathcal{D}u|$). Note that if $u \in W^{1,1}(\Omega)$, then $u \in BV(\Omega)$ and $|\mathcal{D}u|(\Omega) =$

$\int_\Omega |\nabla u| \mathrm{d}x$, where $\nabla u$ refers to the weak gradient of $u$. It can be proven that

$$\int_\Omega |\mathcal{D}u| = \sup\left\{ \int_\Omega u \, \mathrm{div}\mathbf{v} \mathrm{d}x \;\middle|\; \mathbf{v} \in C_c^1(\Omega;\mathbb{R}^2),\ |\mathbf{v}(\mathbf{x})|_{\ell^2} \leq 1 \text{ a.e. } \mathbf{x} \in \Omega \right\}, \tag{1.5}$$

where $C_c^1(\Omega;\mathbb{R}^2)$ denotes the set of continuously differentiable functions $u : \Omega \to \mathbb{R}^2$ with compact support in $\Omega$.

**2. The primal formulation.** This section is devoted to the study of a continuous analogue to the splitting and penalty methods in [26] for the minimization of a discrete TV-model. Let $\Omega \subset \mathbb{R}^2$ be an open, bounded image domain with Lipschitz continuous boundary $\partial\Omega$, and $f \in L^2(\Omega)$ is a given noisy image. The continuous primal formulation of the TV-model (also called ROF-model due to the seminal work in [21]) is given by

$$\bar{u} = \operatorname*{arg\,min}_{u \in BV(\Omega)} \left\{ \mathcal{J}_p(u) := \frac{1}{2}\int_\Omega |u-f|^2 + \alpha \int_\Omega |\mathcal{D}u| \right\}, \tag{2.1}$$

where $\alpha$ is a positive constant.

In many papers (see for instance [7, 20, 21, 26, 27]) finite dimensional versions of (2.1) are considered. In this context, splitting techniques introducing a new variable and penalizing (by means of the $\ell_2$-norm) deviations of this new variable from being the gradient of the reconstructed image are proposed. Such a procedure circumvents the difficulties arising from the nonlinearity and the non-differentiability of the regularization term. Moreover, the (local) convergence analysis of associated iteration schemes for the numerical solution benefit from the discrete context, but may lead to resolution-/mesh-dependent convergence. In the context of (2.1), however, a straightforward extension to $L^2(\Omega)$-penalization (rather than the discrete $\ell_2$-penalty) appears no longer suitable as $\mathcal{D}u$ is a measure only. Furthermore, the non-reflexivity of $BV(\Omega)$ challenges the existence of a solution of the reformulation of (2.1) relevant in variable splitting approaches.

**2.1. A primal variable splitting method.** In [1] a primal variable splitting approach in finite dimensions was considered. In this section we want to understand whether this approach can be related to the original problem (2.1) and an associated variable splitting technique relying on $L^2(\Omega)$-penalties. In fact, the function space analogue of the associated subproblem in the variable splitting approach reads

$$\mathcal{E}_n^p(u,\mathbf{p}) := \frac{1}{2}\int_\Omega |u-f|^2 + \alpha\int_\Omega |\mathbf{p}| + \frac{r_n}{2}|\mathbf{p}-\nabla u|^2_{\mathbf{L}^2}, \tag{2.2}$$

where $f \in L^2(\Omega)$ and for each $n \in \mathbb{N}$, we have $\mathcal{E}_n^p : X \to \mathbb{R} \cup \{+\infty\}$ with $X := W^{1,1}(\Omega) \times \mathbf{L}^1(\Omega)$ and $r_n \to +\infty$ for $n \to +\infty$. Since $\mathcal{E}_n^p$ is not coercive and $X$ is not reflexive, existence of a solution to (2.2) cannot be guaranteed for fixed $n$. As a remedy, we rather study the behavior of a sequence $\{(u_n,\mathbf{p}_n)\}$ in $X$ associated with $r_n \uparrow +\infty$. For this purpose, let $(u_n,\mathbf{p}_n)$ satisfy

$$\mathcal{E}_n^p(u_n,\mathbf{p}_n) \leq \inf_{(u,\mathbf{p})\in X} \mathcal{E}_n^p(u,\mathbf{p}) + \epsilon_n, \tag{2.3}$$

for $\epsilon_n > 0$, $n \in \mathbb{N}$, with $\epsilon_n \downarrow 0$.

Let us briefly comment on the choice of $X$ in this context. First of all, $W^{1,1}(\Omega)$ appears somewhat minimal for (2.2) and it is continuously embedded in $BV(\Omega)$. For

$u \in W^{1,1}(\Omega)$ we have $\nabla u \in \mathbf{L}^1(\Omega)$ and $\int_\Omega |\mathcal{D}u| = \int_\Omega |\nabla u|$. We should also note that other penalized unconstrained problems are conceivable for the splitting approach. An example would be

$$BV(\Omega) \times \mathbf{M}(\Omega;\mathbb{R}^2) \ni (u,\mathbf{p}) \mapsto \frac{1}{2}\int_\Omega |u-f|^2 + \alpha|\mathbf{p}|(\Omega) + r_n|\mathbf{p}-\mathcal{D}u|(\Omega). \tag{2.4}$$

In this case, minimizers do exist but the minimization problem is essentially at least as complicated as the original TV-model. Concerning the existence of a solution to (2.4), let $\{(u_k,\mathbf{p}_k)\}$ be an infimizing sequence for (2.4). Then $|\mathbf{p}_k|(\Omega) < \infty$, and hence there exists $\mathbf{p}^* \in \mathbf{M}(\Omega;\mathbb{R}^2)$ such that $\mathbf{p}_k \to \mathbf{p}^*$ (along a subsequence) in the $\sigma(C_c', C_c)$-topology, where $C_c$ and $C_c'$ stand for $C_c(\Omega;\mathbb{R}^2)$ and its dual, respectively. Therefore, we have that $|\mathbf{p}^*|(\Omega) \le \underline{\lim}_{n\to\infty} |\mathbf{p}_k|(\Omega)$. Additionally, $\{u_k\}$ is bounded in $L^2(\Omega)$ (and hence in $L^1(\Omega)$) and $\{\mathcal{D}u_k\}$ is bounded in $\mathbf{M}(\Omega;\mathbb{R}^2)$ (by the boundedness of $\{\mathbf{p}_k\}$), from which we infer that $\{u_k\}$ is bounded in $BV(\Omega)$. This implies that there exists $u^* \in BV(\Omega)$ such that $u_k \rightharpoonup u^*$ in $L^2(\Omega)$ and $\mathcal{D}u_k \to \mathcal{D}u^*$ in the $\sigma(C_c', C_c)$-topology along a suitable subsequence; see Proposition 10.1.1. in [3] and Theorem 10.1.4., in the same reference, for a proof of the compact embedding $BV(\Omega) \hookrightarrow L^1(\Omega)$. Therefore, we have

$$\frac{1}{2}\int_\Omega |u^*-f|^2 + \alpha|\mathbf{p}^*|(\Omega) + r_n|\mathbf{p}^*-\mathcal{D}u^*|(\Omega) \le \underline{\lim}_{n\to\infty} \frac{1}{2}\int_\Omega |u_n-f|^2 + \alpha|\mathbf{p}_n|(\Omega) + r_n|\mathbf{p}_n-\mathcal{D}u_n|(\Omega),$$

i.e., $\{(u^*,\mathbf{p}^*)\}$ is a minimizer of (2.4). Additionally, a similar argument can be used to show that the sequence of minimizers $\{(u_n^*,\mathbf{p}_n^*)\}$ of (2.4), where $r_n \to \infty$, satisfies $u_n^* \rightharpoonup u^{**}$ in $L^2(\Omega)$, $\mathbf{p}_n \to \mathcal{D}u^{**}$ in the $\sigma(C_c', C_c)$- topology, both along a subsequence, where $u^{**} \in BV(\Omega)$ solves the TV-model. However, as noted before, in this variable splitting scheme we have no advantages (neither theoretical nor numerical) over the original TV-formulation.

Now, we return to (2.1) and prove that the minimization problem is associated with asymptotic properties of the functional (2.2).

THEOREM 2.1. *Let $\{(u_n,\mathbf{p}_n)\}$ be the sequence in $X$ defined by* (2.3). *Then, we have*

$$u_n \to \bar{u} \text{ in the } L^2(\Omega)\text{-sense and } \int_\Omega |\mathbf{p}_n| \to \int_\Omega |\mathcal{D}\bar{u}|, \tag{2.5}$$

(*along subsequences*) *as $n \to \infty$, where $\bar{u} \in BV(\Omega)$ is given by* (2.1).

*Proof.* We split the proof into several steps.

*Step 1: The sequence $\{u_n\}$ is bounded in $BV(\Omega)$.* By the definition of $\{(u_n,\mathbf{p}_n)\}$ in (2.3) we have $\mathcal{E}_n^p(u_n,\mathbf{p}_n) \le \mathcal{E}_n^p(0,0) + \epsilon_n = \frac{1}{2}\int_\Omega |f|^2 + \epsilon_n$. Thus, $\{\frac{r_n}{2}|\mathbf{p}_n - \nabla u_n|^2_{\mathbf{L}^2(\Omega)}\}$ is bounded. Also, $r_n \uparrow \infty$ and hence $|\mathbf{p}_n - \nabla u_n|_{\mathbf{L}^2(\Omega)} \to 0$ as $n \to \infty$ and, by Hölder's and the triangle inequalities, $\delta_n := \alpha\int_\Omega |\mathbf{p}_n| - \alpha\int_\Omega |\nabla u_n|$ satisfies $\lim_{n\to\infty}\delta_n = 0$.

From the definition of $\delta_n$ and $(u_n, \mathbf{p}_n)$, we obtain

(2.6)
$$-\delta_n + \frac{1}{2}\int_\Omega |f|^2 = \alpha\left(\int_\Omega |\nabla u_n| - \int_\Omega |\mathbf{p}_n|\right) + \frac{1}{2}\int_\Omega |f|^2$$

(2.7)
$$\geq \alpha\left(\int_\Omega |\nabla u_n| - \int_\Omega |\mathbf{p}_n|\right) + \mathcal{E}_n^p(u_n, \mathbf{p}_n) - \epsilon_n$$

(2.8)
$$= \alpha\int_\Omega |\nabla u_n| + \frac{1}{2}\int_\Omega |u_n - f|^2 + \frac{r_n}{2}|\mathbf{p}_n - \nabla u_n|^2_{\mathbf{L}^2} - \epsilon_n$$

(2.9)
$$\geq \alpha\int_\Omega |\nabla u_n| + \frac{1}{2|\Omega|}\left(\int_\Omega |u_n - f|\right)^2 + \frac{r_n}{2}|\mathbf{p}_n - \nabla u_n|^2_{\mathbf{L}^2} - \epsilon_n$$

(2.10)
$$\geq \alpha\int_\Omega |\nabla u_n| + \frac{1}{2|\Omega|}\left(\int_\Omega |u_n| - \int_\Omega |f|\right)^2 + \frac{r_n}{2}|\mathbf{p}_n - \nabla u_n|^2_{\mathbf{L}^2} - \epsilon_n,$$

where Hölder's inequality yields (2.9) and the reverse triangle inequality (2.10).

Since $\delta_n \to 0$ and $\epsilon_n \downarrow 0$, we find that the sequences

(2.11)
$$\left\{\int_\Omega |u_n|\right\} \quad \text{and} \quad \left\{\int_\Omega |\mathcal{D}u_n|\right\},$$

are bounded (note that $\int_\Omega |\mathcal{D}u_n| = \int_\Omega |\nabla u_n|$ for each $n$, since $u_n \in W^{1,1}(\Omega)$), i.e., $\{u_n\}$ is bounded in $BV(\Omega)$.

*Step 2:* $\underline{\lim}_{n\to\infty} r_n|\mathbf{p}_n - \nabla u_n|^2_{L^2} = 0$. From the definition of $\{(u_n, \mathbf{p}_n)\}$ in (2.3), we have that $\mathcal{E}_n^p(u_n, \mathbf{p}_n) \leq \mathcal{E}_n^p(u, \nabla u) + \epsilon_n$ for any $u \in W^{1,1}(\Omega)$, i.e.,

(2.12)
$$\frac{1}{2}\int_\Omega |u_n - f|^2 + \alpha\int_\Omega |\mathbf{p}_n| + \frac{r_n}{2}|\mathbf{p}_n - \nabla u_n|^2_{\mathbf{L}^2} \leq \frac{1}{2}\int_\Omega |u - f|^2 + \alpha\int_\Omega |\nabla u| + \epsilon_n.$$

From the definition of $\delta_n$, we get $\alpha\int_\Omega |\mathbf{p}_n| = \delta_n + \alpha\int_\Omega |\nabla u_n|$. Since $\{u_n\}$ is bounded in $BV(\Omega)$ and, thus, in $L^2(\Omega)$ (recall that $BV(\Omega) \hookrightarrow L^2(\Omega)$; see [2]) there is $\bar{u} \in BV(\Omega)$ for which $u_n \rightharpoonup \bar{u}$ in $L^2(\Omega)$, along a subsequence. Since the embedding $BV(\Omega) \hookrightarrow L^1(\Omega)$ is compact (see [11]), we observe that $u_n \to \bar{u}$ in $L^1(\Omega)$ (along a subsequence of $\{u_n\}$ which we also denote by $\{u_n\}$). This implies $\int_\Omega |\mathcal{D}\bar{u}| \leq \underline{\lim}_{n\to\infty}\int_\Omega |\nabla u_n|$. Thus, we have $\int_\Omega |\mathcal{D}\bar{u}| \leq \underline{\lim}_{n\to\infty}\int_\Omega |\mathbf{p}_n|$ and therefore

(2.13)
$$\frac{1}{2}\int_\Omega |\bar{u} - f|^2 + \alpha\int_\Omega |\mathcal{D}\bar{u}| + a \leq \underline{\lim}_{n\to\infty}\left(\frac{1}{2}\int_\Omega |u_n - f|^2 + \alpha\int_\Omega |\mathbf{p}_n| + \frac{r_n}{2}|\mathbf{p}_n - \nabla u_n|^2_{\mathbf{L}^2}\right),$$

where $a = \underline{\lim}_{n\to\infty} \frac{r_n}{2}|\mathbf{p}_n - \nabla u_n|^2_{\mathbf{L}^2}$. Here we have used the weak lower semicontinuity of the norm and elementary properties of $\underline{\lim}$. Therefore, from (2.12), we infer

(2.14)
$$0 \leq \frac{1}{2}\int_\Omega |\bar{u} - f|^2 + \alpha\int_\Omega |\mathcal{D}\bar{u}| + a \leq \frac{1}{2}\int_\Omega |u - f|^2 + \alpha\int_\Omega |\nabla u|,$$

for all $u \in W^{1,1}(\Omega)$.

Since $\bar{u} \in BV(\Omega) \cap L^2(\Omega)$, one can argue the existence of $\{v_k\} \subset C^\infty(\bar{\Omega}) \subset W^{1,1}(\Omega)$ such that $\lim_{k\to\infty}|v_k - \bar{u}|_{L^2} = 0$ and $\lim_{k\to\infty}\int_\Omega |\nabla v_k| = \int_\Omega |\mathcal{D}\bar{u}|$ (see for

example [4]). We choose $u = v_k$ in the inequality (2.14) and take the limit as $k \to \infty$ to obtain $a = \underline{\lim}_{n\to\infty} \frac{r_n}{2}|\mathbf{p}_n - \nabla u_n|^2_{L^2(\Omega)} = 0$.

*Step 3: $\bar{u} \in BV(\Omega)$ is the minimizer.* Finally, since $a = 0$ in (2.14), we have that

$$\frac{1}{2}\int_\Omega |\bar{u} - f|^2 + \alpha \int_\Omega |\mathcal{D}\bar{u}| \leq \frac{1}{2}\int_\Omega |w - f|^2 + \alpha \int_\Omega |\mathcal{D}w|$$

for all $w \in BV(\Omega)$ by using the same density argument as in the preceding paragraph, i.e., $\bar{u}$ is a minimizer of the TV-model.

*Step 4: $u_n \to \bar{u}$ in the $L^2(\Omega)$-sense and $\int_\Omega |\mathbf{p}_n| \to \int_\Omega |\mathcal{D}\bar{u}|$ (along subsequences).* Using $a = \underline{\lim}_{n\to\infty} \frac{r_n}{2}|\mathbf{p}_n - \nabla u_n|^2_{\mathbf{L}^2} = 0$ and the inequalities in (2.12) and (2.13), we obtain that

$$\underline{\lim}_{n\to\infty} \left(\frac{1}{2}\int_\Omega |u_n - f|^2 + \alpha \int_\Omega |\mathbf{p}_n|\right) = \frac{1}{2}\int_\Omega |\bar{u} - f|^2 + \alpha \int_\Omega |\mathcal{D}\bar{u}|, \tag{2.15}$$

where the density argument of Step 3 has been used. Then, we consider a subsequence of $\{(u_n, \mathbf{p}_n)\}$ (again denoted by $\{(u_n, \mathbf{p}_n)\}$) for which the previous relation holds when "$\underline{\lim}$" is replaced by "lim". From the previous steps, we know that $\int_\Omega |\bar{u} - f|^2 \leq \underline{\lim}_{n\to\infty} \int_\Omega |u_n - f|^2$, due to $u_n \rightharpoonup \bar{u}$ in the $L^2(\Omega)$-sense, and $\int_\Omega |\mathcal{D}\bar{u}| \leq \underline{\lim}_{n\to\infty} \int_\Omega |\mathbf{p}_n|$. Hence, we have $-\underline{\lim}_{n\to\infty} \int_\Omega |\mathbf{p}_n| \leq -\int_\Omega |\mathcal{D}\bar{u}|$ and equivalently $\overline{\lim}_{n\to\infty} \int_\Omega (-|\mathbf{p}_n|) \leq -\int_\Omega |\mathcal{D}\bar{u}|$. Therefore, we obtain

$$\frac{1}{2}\int_\Omega |\bar{u} - f|^2 \leq \underline{\lim}_{n\to\infty} \frac{1}{2}\int_\Omega |u_n - f|^2 \tag{2.16}$$

$$= \underline{\lim}_{n\to\infty} \left(\frac{1}{2}\int_\Omega |u_n - f|^2 + \alpha \int_\Omega |\mathbf{p}_n| - \alpha \int_\Omega |\mathbf{p}_n|\right) \tag{2.17}$$

$$\leq \overline{\lim}_{n\to\infty} \left(\frac{1}{2}\int_\Omega |u_n - f|^2 + \alpha \int_\Omega |\mathbf{p}_n| - \alpha \int_\Omega |\mathbf{p}_n|\right) \tag{2.18}$$

$$\leq \frac{1}{2}\int_\Omega |\bar{u} - f|^2 + \alpha \int_\Omega |\mathcal{D}\bar{u}| + \overline{\lim}_{n\to\infty} \left(-\alpha \int_\Omega |\mathbf{p}_n|\right) \tag{2.19}$$

$$\leq \frac{1}{2}\int_\Omega |\bar{u} - f|^2 + \alpha \int_\Omega |\mathcal{D}\bar{u}| - \alpha \int_\Omega |\mathcal{D}\bar{u}| \tag{2.20}$$

$$= \frac{1}{2}\int_\Omega |\bar{u} - f|^2. \tag{2.21}$$

Hence, $\underline{\lim}_{n\to\infty} \int_\Omega |u_n - f|^2 = \int_\Omega |\bar{u} - f|^2$, and along a subsequence of $\{u_n\}$ we have $\int_\Omega |u_n - f|^2 \to \int_\Omega |\bar{u} - f|^2$. We also have $(u_n - f) \rightharpoonup (\bar{u} - f)$ in $L^2(\Omega)$. Therefore, as $L^2(\Omega)$ is a locally uniformly convex space, $(u_n - f) \to (\bar{u} - f)$ in $L^2(\Omega)$ and hence $|u_n - \bar{u}|_{L^2} \to 0$ along a subsequence.

Finally, since we have

$$\lim_{n\to\infty} \left(\frac{1}{2}\int_\Omega |u_n - f|^2 + \alpha \int_\Omega |\mathbf{p}_n|\right) = \frac{1}{2}\int_\Omega |\bar{u} - f|^2 + \alpha \int_\Omega |\mathcal{D}\bar{u}|, \tag{2.22}$$

and $(u_n - f) \to (\bar{u} - f)$ in $L^2(\Omega)$ along a subsequence of $\{(u_n, \mathbf{p}_n)\}$, we have that $\lim_{n\to\infty} \int_\Omega |\mathbf{p}_n| = \int_\Omega |\mathcal{D}\bar{u}|$. □

Note that the penalized problem (2.2) can be formally related to the constrained optimization problem

$$\text{Minimize } \mathcal{J}_p(u, \mathbf{p}) := \frac{1}{2}|u - f|^2_{L^2} + \alpha|\mathbf{p}|_{\mathbf{L}^1} \quad \text{over } (u, \mathbf{p}) \in X, \tag{2.23}$$

$$\text{s.t.} \quad g(u, \mathbf{p}) := \nabla u - \mathbf{p} = 0, \tag{2.24}$$

where "s.t." stands for "subject to". In finite dimensions, augmented Lagrangian methods have been applied successfully for image reconstruction over the recent years; see for example [7, 16, 27]. However, in the infinite dimensional case many obstacles arise, not only of theoretical nature but also associated with the numerical implementation of the problem. For example, the functional $X \ni (u, \mathbf{p}) \mapsto \mathcal{J}_p(u, \mathbf{p})$ is not differentiable and Lagrange multipliers might not exist. On the other hand, the following theorem contains a generalization in the case we consider a "pseudo augmented Lagrangian", where the elements taking the role of Lagrange multipliers are regular objects.

Consider the sequences $\{r_n\}$ in $\mathbb{R}^+$ and $\{\boldsymbol{\lambda}_n\}$ in $\mathbf{L}^2(\Omega)$ and suppose that $\{r_n\}$ is monotonically increasing, $\lim_{n\to\infty} r_n \to \infty$ and $\sup_{n\in\mathbb{N}} |\boldsymbol{\lambda}_n|_{\mathbf{L}^2} < \infty$. For each $n \in \mathbb{N}$, consider the extended real-valued functional $\mathcal{L}^p_{r_n} : X \times \mathbf{L}^2(\Omega) \to \mathbb{R} \cup \{+\infty\}$, where $X = W^{1,1}(\Omega) \times \mathbf{L}^1(\Omega)$, defined by

(2.25)
$$\mathcal{L}^p_{r_n}(u, \mathbf{p}, \boldsymbol{\lambda}_n) = \frac{1}{2}\int_\Omega |u - f|^2 + \alpha \int_\Omega |\mathbf{p}| + \frac{r_n}{2}\int_\Omega |\mathbf{p} - \nabla u|^2 + \int_\Omega \boldsymbol{\lambda}_n \cdot (\mathbf{p} - \nabla u)\,.$$

Similarly as before, we consider a sequence $\{(u_n, \mathbf{p}_n)\}$ in $X$ of $\epsilon$-minimizers of $(u, \mathbf{p}) \mapsto \mathcal{L}^p_{r_n}(u, \mathbf{p}, \boldsymbol{\lambda})$. Let $\{\epsilon_n\}$ satisfy $\epsilon_n > 0$ for all $n \in \mathbb{N}$ and $\epsilon_n \downarrow 0$. Moreover, for a fixed $n$ let $(u_n, \mathbf{p}_n)$ be such that

$$\mathcal{L}^p_{r_n}(u_n, \mathbf{p}_n, \boldsymbol{\lambda}_n) \leq \inf_{(u,\mathbf{p})\in X} \mathcal{L}^p_{r_n}(u, \mathbf{p}, \boldsymbol{\lambda}_n) + \epsilon_n. \tag{2.26}$$

We observe that the sequence $\{(u_n, \mathbf{p}_n)\}$ is well-defined since $(u, \mathbf{p}) \mapsto \mathcal{L}^p_{r_n}(u, \mathbf{p}, \boldsymbol{\lambda}_n)$ is bounded from below. For the sake of brevity suppose that $r_n \geq 1$. Then, completing squares in the last two terms of $\mathcal{L}^p_{r_n}$, we obtain $\mathcal{L}^p_{r_n}(u, \mathbf{p}, \boldsymbol{\lambda}_n) \geq -|\boldsymbol{\lambda}_n|_{\mathbf{L}^2} \geq -\sup_{n\in\mathbb{N}} |\boldsymbol{\lambda}_n|_{\mathbf{L}^2} > -\infty$. We are now in a position to prove the analogue to Theorem 2.1 but for the functional $\mathcal{L}^p_{r_n}$.

THEOREM 2.2. *Let $\{(u_n, \mathbf{p}_n)\}$ be the sequence defined by* (2.26)*. Then the same conclusion of Theorem 2.1 holds.*

*Proof.* The proof is split into several steps.

*Step 1: The sequence $\{u_n\}$ is bounded in $BV(\Omega)$.* By the definition of $\{(u_n, \mathbf{p}_n)\}$ we have $\mathcal{L}^p_{r_n}(u_n, \mathbf{p}_n, \boldsymbol{\lambda}_n) \leq \mathcal{L}^p_{r_n}(0, 0, \boldsymbol{\lambda}_n) + \epsilon_n$. Then, upon completing squares, we find that $r_n|\mathbf{p}_n - \nabla u_n|^2_{\mathbf{L}^2}$ is bounded by (2.25). This implies $\lim_{n\to\infty} |\mathbf{p}_n - \nabla u_n|_{\mathbf{L}^2} = 0$ and $\lim_{n\to\infty} \langle \boldsymbol{\lambda}_n, \mathbf{p}_n - \nabla u_n\rangle_{\mathbf{L}^2} = 0$. Then, arguing as in Step 1 of the proof of Theorem 2.1, we obtain

$$\begin{aligned} &-\delta_n + \frac{1}{2}\int_\Omega |f|^2 \geq \\ &\alpha \int_\Omega |\nabla u_n| + \frac{1}{2|\Omega|}\left(\int_\Omega |u_n| - \int_\Omega |f|\right)^2 + \frac{r_n}{2}|\mathbf{p}_n - \nabla u_n|^2_{L^2(\Omega)} + \langle \boldsymbol{\lambda}_n, \mathbf{p}_n - \nabla u_n\rangle_{\mathbf{L}^2} - \epsilon_n, \end{aligned}$$

where $\delta_n = \alpha(\int_\Omega |\mathbf{p}_n| - \int_\Omega |\nabla u_n|)$. The latter expression tends to zero as $n \to \infty$ since $\lim_{n\to\infty} |\mathbf{p}_n - \nabla u_n|_{\mathbf{L}^2} = 0$. Hence, as $\epsilon_n \downarrow 0$ we have that the sequences

$$\left\{\int_\Omega |u_n|\right\} \quad \text{and} \quad \left\{\int_\Omega |\mathcal{D}u_n|\right\}, \tag{2.27}$$

are bounded. Thus, we conclude that $\{u_n\}$ in $W^{1,1}(\Omega)$ is bounded in $BV(\Omega)$.

*Step 2:* $\underline{\lim}_{n\to\infty} r_n|\mathbf{p}_n - \nabla u_n|^2_{L^2} = 0$*, existence of a minimizer and appropriate convergence.* From the definition of $\{(u_n, \mathbf{p}_n)\}$, we infer $\mathcal{L}^p_{r_n}(u_n, \mathbf{p}_n, \boldsymbol{\lambda}_n) \le \mathcal{L}^p_{r_n}(u, \nabla u, \boldsymbol{\lambda}_n) + \epsilon_n$ for any $u \in W^{1,1}(\Omega)$. Since we know that $\lim_{n\to\infty}\langle \boldsymbol{\lambda}_n, \mathbf{p}_n - \nabla u_n\rangle_{\mathbf{L}^2} = 0$, we argue as in the Step 2 of the proof of Theorem 2.1 and obtain a subsequence of $\{u_n\}$ ( also denoted by $\{u_n\}$) and $\bar{u} \in BV(\Omega)$ such that $u_n \rightharpoonup \bar{u}$ in $L^2(\Omega)$ and $\int_\Omega |\mathcal{D}u| \le \underline{\lim}_{n\to\infty} \int_\Omega |\nabla u_n|$. Then, $\int_\Omega |\mathcal{D}u| \le \underline{\lim}_{n\to\infty} \int_\Omega |\mathbf{p}_n|$ due to $\delta_n = \alpha(\int_\Omega |\mathbf{p}_n| - \int_\Omega |\nabla u_n|)$ going to 0 as $n \to \infty$, and we observe

$$0 \le \frac{1}{2}\int_\Omega |\bar{u} - f|^2 + \alpha \int_\Omega |\mathcal{D}\bar{u}| + a \le \frac{1}{2}\int_\Omega |u - f|^2 + \alpha \int_\Omega |\nabla u|, \tag{2.28}$$

where $a = \underline{\lim}_{n\to\infty} \frac{r_n}{2}|\mathbf{p}_n - \nabla u_n|^2_{L^2(\Omega)}$. A density argument analogous to the one at the end of Step 2 and Step 3 of the proof of Theorem 2.1 implies that $a = 0$ and consequently that $\bar{u}$ is a minimizer of the TV-model. Finally, Step 4 in the proof of Theorem 2.1 is valid here and the assertion follows. □

**2.1.1. The Discrete Augmented Lagrangian.** For the sake of keeping this paper self-contained, we briefly specify the augmented Lagrangian method associated with a discrete version of (2.23)-(2.24). For details see, e.g., [20, 27]. Given a penalty parameter $r_n > 0$ and an (approximate) multiplier $\boldsymbol{\lambda}$, the discrete augmented Lagrangian reads

$$\begin{aligned}\mathcal{L}^p_{n,h}(u, \mathbf{p}, \boldsymbol{\lambda}) := h^2 \sum_{(i,j)\in\Omega_h} &\frac{1}{2}|u_{i,j} - f_{i,j}|^2 + \alpha|\mathbf{p}_{i,j}| + \frac{r_n}{2}|\mathbf{p}_{i,j} - (\nabla_h u)_{i,j}|^2 \\ &+ \boldsymbol{\lambda}_{i,j} \cdot (\mathbf{p}_{i,j} - (\nabla_h u)_{i,j}),\end{aligned} \tag{2.29}$$

where $\mathcal{L}^p_{n,h} : X_h \to \mathbb{R} \cup \{\infty\}$ with $X_h := \mathbb{R}^{N^2} \times \mathbb{R}^{2N^2} \times \mathbb{R}^{2N^2}$.

In Algorithm 1, an alternating minimization algorithm (see [20, 27]) for the augmented Lagrangian is implemented. For a fixed penalty parameter $r_n$, the "suitable stopping criteria" in step 5 of Algorithm 1 may be identified with residuals of the first-order optimality conditions dropping below a specified tolerance. As a soft-thresholding technique provides an explicit solution which satisfies the first-order optimality condition of the $\mathbf{p}$-subproblem in step 3, it suffices to check whether the residual of the first-order optimality condition of the $u$-subproblem step 2, i.e.,

$$\mathbf{R}^k_{n,h} := r_n \mathrm{div}_h(\mathbf{p}^k_{n,h} - \nabla_h u^k_{n,h}) + \mathrm{div}_h \boldsymbol{\lambda}^k_{n,h} + u^k_{n,h} - f, \tag{2.30}$$

is sufficiently small.

It is known (see [27] for a proof) that for any finite positive penalty parameter $r_n > 0$, a sequence $\{(u^k_{n,h}, \mathbf{p}^k_{n,h}, \boldsymbol{\lambda}^k_{r,h})\}_{k\in\mathbb{N}}$ (generated by Algorithm 1) converges to a saddle point of $\mathcal{L}^p_{n,h}(u, \mathbf{p}, \boldsymbol{\lambda})$, as $k \to \infty$. Moreover the limit point of $\{u^k_{n,h}\}$ is a minimizer of the discrete ROF/TV-functional. In addition, the algorithm is equivalent to the split Bregman method; see [12]. However, it is not straightforward to obtain the same results (in terms of the convergence of the algorithm) in infinite dimensions. For example, it is not clear whether the Lagrange multiplier (in case it exists at all) is regular enough to have a pointwise description. Consequently, the update in step 2 of Algorithm 1 might no longer be appropriate.

**3. The Fenchel pre-dual formulation.** In this section, we propose algorithms for finding a solution of the TV-model (2.1) from its Fenchel pre-dual formulation:

$$\bar{\mathbf{s}} = \operatorname*{arg\,min}_{\mathbf{s}\in H_0(\mathrm{div})} \left\{ \mathcal{J}_d(\mathbf{s}) := \frac{1}{2}\,|\mathrm{div}\mathbf{s} + f|^2_{L^2} \quad \text{s.t} \quad |\mathbf{s}(\mathbf{x})|_{\ell^2} \le \alpha \text{ a.e. } \mathbf{x} \in \Omega \right\}, \tag{3.1}$$

**Algorithm 1** (Discrete Primal Augmented Lagrangian)

1: **Initialization.** Choose $(\mathbf{p}^0_{n,h}, \boldsymbol{\lambda}^0_{n,h})$ and set $k := 1$.
2: **Compute**

$$u^k_{n,h} \in \arg\min_u \sum_{(i,j)\in\Omega_h} \frac{1}{2}|u_{i,j} - f_{i,j}|^2 + \frac{r_n}{2}\left|\left(\mathbf{p}^{k-1}_{n,h}\right)_{i,j} - (\nabla_h u)_{i,j}\right|^2 - \left(\boldsymbol{\lambda}^{k-1}_{n,h}\right)_{i,j} \cdot (\nabla_h u)_{i,j}\,.$$

3: **Compute**

$$\mathbf{p}^k_{n,h} \in \arg\min_{\mathbf{p}} \sum_{(i,j)\in\Omega_h} \alpha|\mathbf{p}_{i,j}| + \frac{r_n}{2}\left|\mathbf{p}_{i,j} - \left(\nabla_h u^k_{n,h}\right)_{i,j}\right|^2 + \left(\boldsymbol{\lambda}^{k-1}_{n,h}\right)_{i,j} \cdot \mathbf{p}_{i,j}.$$

4: **Set**

$$\left(\boldsymbol{\lambda}^k_{n,h}\right)_{i,j} := \left(\boldsymbol{\lambda}^{k-1}_{n,h}\right)_{i,j} + r_n\left(\left(\mathbf{p}^k_{n,h}\right)_{i,j} - \left(\nabla_h u^k_{n,h}\right)_{i,j}\right), \quad (i,j) \in \Omega_h.$$

5: **Check stopping criteria.** If suitable stopping criteria are met, $(u^*_{n,h}, \mathbf{p}^*_{n,h}, \boldsymbol{\lambda}^*_{n,h}) = (u^k_{n,h}, \mathbf{p}^k_{n,h}, \boldsymbol{\lambda}^k_{n,h})$; otherwise set $k := k + 1$ and return to step 2.

where $\mathrm{div} \in \mathscr{L}(H_0(\mathrm{div}), L^2(\Omega))$, with

$$H_0(\mathrm{div}) = \left\{\mathbf{s} \in \mathbf{L}^2(\Omega) \,:\, \mathrm{div}\mathbf{s} \in L^2(\Omega),\, \mathbf{s}\cdot\nu = 0 \text{ on } \partial\Omega\right\},$$

and $\nu$ is the outward unit normal vector on $\partial\Omega$. For more information on (3.1) and associated solvers see [14] and [8]. A solution of the TV-model (2.1) is obtained from $\bar{\mathbf{s}}$ by

$$\bar{u} = \mathrm{div}\bar{\mathbf{s}} + f \quad \text{in} \quad \Omega. \tag{3.2}$$

A main feature of the minimization problem (3.1) is that a minimizer need not be unique. In [14] an orthogonal projection in $\mathbf{L}^2(\Omega)$ onto $\{\mathbf{s} \in H_0(\mathrm{div}) : \mathrm{div}\mathbf{s} = 0 \text{ a.e. in } \Omega\}$ is used in order to avoid non-uniqueness of the solution in (3.1). In [15] a Tikhonov-type regularization in $H^1_0(\Omega)$ is considered as a remedy. In the aforementioned paper it is shown that the Tikhonov regularization in the pre-dual formulation (3.1) changes the TV-regularization in the primal formulation (2.1) into a local Huber-type regularization.

In recent years, algorithms operating on the (pre-)dual formulation of the TV-model have become popular; see, e.g., [5, 14, 15]. While in finite dimensions, the dual problem equals the pre-dual, this is not the case in infinite dimensions. The latter fact is a consequence of the non-reflexivity of $BV(\Omega)$.

The primal-dual algorithms in [14, 15] in the infinite dimensional setting exhibit local superlinear convergence. However, in order to obtain a solution of the TV-model, the Tikhonov-regularization parameter needs to vanish. For a positive regularization parameter, the iterates of the previous algorithm remain in a space more regular than $BV(\Omega)$.

In finite dimensions, an algorithm for computing a minimizer of a discretized version of $\mathcal{J}_d$ in (3.1) is proposed in [5], where its conditional convergence is also proved. In [6], an upwind finite-difference method for the discretized $\mathcal{J}_d$ is introduced and shown to reduce anisotropy of the reconstruction, which occurs if standard diffusion schemes are used. However, it is not straightforward to extend the algorithms proposed in [5,6] into infinite dimensional spaces.

**3.1. A variable splitting method.** In this and the next section we study variable splitting and augmented Lagrangian methods in function space, respectively. For this purpose let $\mathcal{R} \subset \mathbf{L}^2(\Omega)$ be defined as

$$\mathcal{R} := \{\mathbf{t} \in \mathbf{L}^2(\Omega) \,:\, |\mathbf{t}(\mathbf{x})| \leq \alpha \text{ a.e. } \mathbf{x} \in \Omega\} \tag{3.3}$$

and let $\delta_{\mathcal{R}}$ denote the indicator function

$$\delta_{\mathcal{R}}(\mathbf{t}) = \begin{cases} 0 & \mathbf{t} \in \mathcal{R}, \\ +\infty & \text{otherwise.} \end{cases} \tag{3.4}$$

Consider the following problem

$$\text{Minimize } \mathcal{E}_n^d(\mathbf{s},\mathbf{t}) := \frac{1}{2}|\mathrm{div}\mathbf{s} + f|_{L^2}^2 + \frac{q_n}{2}|\mathbf{s}-\mathbf{t}|_{L^2}^2 + \delta_{\mathcal{R}}(\mathbf{t}) \quad \text{over } (\mathbf{s},\mathbf{t}) \in Y, \tag{3.5}$$

where $Y := H_0(\mathrm{div}) \times \mathbf{L}^2(\Omega)$ and $\mathcal{E}_n^d : Y \to \mathbb{R} \cup \{+\infty\}$. It is next shown that minimizers of $\mathcal{E}_n^d$ are closely related to problem (3.1) for $n \to \infty$, provided that $\lim_{n\to\infty} q_n = \infty$.

LEMMA 3.1. *For each $n \in \mathbb{N}$, there exists a minimizer $(\mathbf{s}_n, \mathbf{t}_n)$ of $\mathcal{E}_n^d : H_0(\mathrm{div}) \times \mathbf{L}^2(\Omega) \to \mathbb{R}$. For $q_n \to \infty$ as $n \to \infty$, one further has $\mathbf{s}_n \rightharpoonup \mathbf{s}^*$ (along a subsequence) in $H_0(\mathrm{div})$ as $n \to \infty$, where $\mathbf{s}^*$ is a solution to (3.1).*

*Proof.* If $\mathbf{t} \notin \mathcal{R}$, then $\mathcal{E}_n^d(\mathbf{s},\mathbf{t}) = \infty$. Hence, it suffices to consider the constrained minimization problem

$$\text{Minimize } \mathcal{E}_n^d(\mathbf{s},\mathbf{t}) \quad \text{over } (\mathbf{s},\mathbf{t}) \in Y_{\mathcal{R}}, \tag{3.6}$$

where $Y_{\mathcal{R}} := H_0(\mathrm{div}) \times \mathcal{R} \subset Y$.

We first note that $\mathcal{E}_n^d$ is convex and coercive on $Y_{\mathcal{R}}$. Indeed, the functional $H_0(\mathrm{div}) \ni \mathbf{s} \mapsto |\mathrm{div}\mathbf{s} + f|_{L^2}^2$ is convex since $\mathrm{div} \in \mathscr{L}(H_0(\mathrm{div}), L^2(\Omega))$ and the squared norm $|\cdot|_{L^2}^2$ is convex. Further, consider $Y_{\mathcal{R}} \ni \mathbf{r} := (\mathbf{s},\mathbf{t}) \mapsto |\mathbf{s}-\mathbf{t}|_{L^2}^2 =: \mathcal{P}(\mathbf{r})$. Then for $\mathbf{r}_1, \mathbf{r}_2 \in Y_{\mathcal{R}}$ and $\lambda \in [0,1]$ we find

$$\begin{aligned} \mathcal{P}(\lambda\mathbf{r}_1 + (1-\lambda)\mathbf{r}_2) &= |\lambda\mathbf{s}_1 + (1-\lambda)\mathbf{s}_2 - (\lambda\mathbf{t}_1 + (1-\lambda)\mathbf{t}_2)|_{L^2}^2 \\ &= |\lambda(\mathbf{s}_1 - \mathbf{t}_1) + (1-\lambda)(\mathbf{s}_2 - \mathbf{t}_2)|_{L^2}^2 \\ &\leq \lambda\mathcal{P}(\mathbf{r}_1) + (1-\lambda)\mathcal{P}(\mathbf{r}_2); \end{aligned}$$

Combining both arguments above yields the convexity of $\mathcal{E}_n^d$. By the reversed triangle inequality, we have

$$\mathcal{E}_n^d(\mathbf{s},\mathbf{t}) \geq \frac{1}{2}(|\mathrm{div}\mathbf{s}|_{L^2} - |f|_{L^2})^2 + \frac{q_n}{2}(|\mathbf{s}|_{\mathbf{L}^2} - |\mathbf{t}|_{\mathbf{L}^2})^2. \tag{3.7}$$

Hence, if the sequence $\{(\mathbf{s}_k,\mathbf{t}_k)\}$ in $Y_{\mathcal{R}} \subset Y$ is unbounded, then $\{\mathbf{s}_k\}$ is unbounded in $H_0(\mathrm{div})$ as $\{\mathbf{t}_k\}$ is in $\mathcal{R}$ (a bounded subset of $\mathbf{L}^2(\Omega)$). Thus, for $|\mathbf{s}_k|_{H_0(\mathrm{div})} \to \infty$, we get hence $\mathcal{E}_n^d(\mathbf{s}_k,\mathbf{t}_k) \to \infty$, i.e., $\mathcal{E}_n^d$ is coercive.

It follows directly that $\mathcal{E}_n^d$ is continuous (and convex from the previous paragraph), and since $Y_{\mathcal{R}} \subset Y$ is closed, $\mathcal{E}_n^d$ is weakly lower semicontinuous over $Y_{\mathcal{R}}$. Since $Y$ is reflexive, the problem in (3.6) has a solution and consequently, for each $n \in \mathbb{N}$, $\mathcal{E}_n^d$ has minimizers over $Y$.

For the sake of simplicity assume that $q_n \leq q_{n+1}$ for $n \in \mathbb{N}$ (otherwise we can extract a non-decreasing subsequence). For $n \in \mathbb{N}$, let $(\mathbf{s}_n^*, \mathbf{t}_n^*) \in Y$ be a minimizer of $\mathcal{E}_n^d$. Then, we infer $\frac{1}{2}|f|_{L^2}^2 = \mathcal{E}_n^d(0,0) \geq \mathcal{E}_n^d(\mathbf{s}_n^*, \mathbf{t}_n^*)$ and $\mathcal{E}_n^d(\mathbf{s}_n^*, \mathbf{t}_n^*) \leq \mathcal{E}_n^d(\mathbf{s}_{n+1}^*, \mathbf{t}_{n+1}^*) \leq \mathcal{E}_{n+1}^d(\mathbf{s}_{n+1}^*, \mathbf{t}_{n+1}^*)$ for all $n \in \mathbb{N}$, from standard arguments for penalty functions (see [19]) we have that $\lim_{n\to\infty} \frac{q_n}{2}|\mathbf{s}_n^* - \mathbf{t}_n^*|_{\mathbf{L}^2}^2 = 0$.

Since $\{\mathbf{t}_n^*\}$ in $\mathcal{R}$ is bounded in $\mathbf{L}^2(\Omega)$ and $\frac{1}{2}|f|_{L^2}^2 \geq \mathcal{E}_n^d(\mathbf{s}_n^*, \mathbf{t}_n^*)$, from the coercivity of $\mathcal{E}_n^d$ we obtain that $\{\mathbf{s}_n^*\}$ is bounded in $H_0(\mathrm{div})$. Thus, there exists a subsequence of $\{(\mathbf{s}_n^*, \mathbf{t}_n^*)\}$ (again denoted by $\{(\mathbf{s}_n^*, \mathbf{t}_n^*)\}$) for which $(\mathbf{s}_n^*, t_n^*) \rightharpoonup (\mathbf{s}^*, \mathbf{t}^*)$ in $H_0(\mathrm{div}) \times \mathbf{L}^2(\Omega)$ as $n \to \infty$. Now, let $\mathbf{s} \in \mathcal{R} \cap H_0(\mathrm{div})$ be arbitrary, but fixed. Then

$$\frac{1}{2}|\mathrm{div}\mathbf{s} + f|_{L^2}^2 = \mathcal{E}_n^d(\mathbf{s}, \mathbf{s}) \geq \mathcal{E}_n^d(\mathbf{s}_n^*, \mathbf{t}_n^*) \geq \frac{1}{2}|\mathrm{div}\mathbf{s}_n^* + f|_{L^2}^2 + \frac{q_n}{2}|\mathbf{s}_n^* - \mathbf{t}_n^*|_{\mathbf{L}^2}^2.$$

Using the weakly lower semicontinuity of the norm and $\lim_{n\to\infty} \frac{q_n}{2}|\mathbf{s}_n^* - \mathbf{t}_n^*|_{\mathbf{L}^2}^2 = 0$, we obtain

$$\frac{1}{2}|\mathrm{div}\mathbf{s} + f|_{L^2}^2 \geq \frac{1}{2}|\mathrm{div}\mathbf{s}^* + f|_{L^2}^2.$$

Since $\lim_{n\to\infty} |\mathbf{s}_n^* - \mathbf{t}_n^*|_{\mathbf{L}^2} = 0$ and $\mathbf{t}^* \in \mathcal{R}$, we have $\mathbf{s}^* \in \mathcal{R} \cap H_0(\mathrm{div})$. Finally, as $\mathbf{s} \in \mathcal{R} \cap H_0(\mathrm{div})$ was arbitrary, $\mathbf{s}^*$ is a solution to (3.1). □

*Remark.* The result in the previous theorem can be strengthened. In fact, besides $\mathbf{s}_n^* \rightharpoonup \mathbf{s}^*$ in $H_0(\mathrm{div})$, one also has $\mathrm{div}\mathbf{s}_n^* \to \mathrm{div}\mathbf{s}^*$ in $L^2(\Omega)$. However, whether $\mathbf{s}_n^* \to \mathbf{s}^*$ in $H_0(\mathrm{div})$, remains an open question.

In order to study the convergence of the splitting algorithm, we introduce the following auxiliary problems. For $0 < \eta < 1$ let $\mathcal{G}_n, \mathcal{G}_n^\eta : H_0(\mathrm{div}) \to \mathbb{R}$ be defined by $\mathcal{G}_n(\mathbf{s}) := \mathcal{E}_n^d(\mathbf{s}, P_{\mathcal{R}}(\mathbf{s}))$ and $\mathcal{G}_n^\eta(\mathbf{s}) := \mathcal{E}_n^d(\mathbf{s}, \eta P_{\mathcal{R}}(\mathbf{s}))$, where $P_{\mathcal{R}}(\mathbf{s})$ is the $\mathbf{L}^2(\Omega)$-projection of $\mathbf{s}$ onto $\mathcal{R}$, i.e.,

(3.8)
$$\mathcal{G}_n(\mathbf{s}) = \frac{1}{2}|\mathrm{div}\mathbf{s} + f|_{L^2}^2 + \frac{q_n}{2}|\mathbf{s} - P_{\mathcal{R}}(\mathbf{s})|_{\mathbf{L}^2}^2, \quad \mathcal{G}_n^\eta(\mathbf{s}) = \frac{1}{2}|\mathrm{div}\mathbf{s} + f|_{L^2}^2 + \frac{q_n}{2}|\mathbf{s} - \eta P_{\mathcal{R}}(\mathbf{s})|_{\mathbf{L}^2}^2.$$

We utilize an alternating algorithm for approximating minimizers of (3.5). For this purpose, we introduce a new family of problems. For the sake of simplicity take $q \geq 1$ and let $0 < \eta < 1$ be fixed, and consider the sequence $\{\mathbf{s}_\eta^k\}_{k=1}^\infty$ in $H_0(\mathrm{div})$ generated by Algorithm 2. Then, the following theorem establishes a relation between $\{\mathbf{s}_\eta^k\}_{k=1}^\infty$ and the minimizers of $\mathcal{G}_n$ and $\mathcal{G}_n^\eta$.

THEOREM 3.2. *Suppose that $n \in \mathbb{N}$ is fixed and consider $H_0(\mathrm{div}) \times \mathbf{L}^2(\Omega) \ni (\mathbf{s}, \mathbf{t}) \mapsto \mathcal{E}_n^d(\mathbf{s}, \mathbf{t})$, $H_0(\mathrm{div}) \ni \mathbf{s} \mapsto \mathcal{G}^d(\mathbf{s}), \mathcal{G}_n^\eta(\mathbf{s})$ as defined in (3.5) and (3.8), respectively, and the sequence $\{\mathbf{s}_\eta^k\}_{k=1}^\infty$ in $H_0(\mathrm{div})$ defined by Algorithm 2 with $q = q_n$. Then the following holds true:*

- **i.** *For each $0 < \eta < 1$, there exists $\mathbf{s}_\eta \in H_0(\mathrm{div})$ such that $\mathbf{s}_\eta^k \to \mathbf{s}_\eta$ in $H_0(\mathrm{div})$ as $k \to \infty$. The map $(0,1) \ni \eta \mapsto \mathbf{s}_\eta \in H_0(\mathrm{div})$ is locally Lipschitz continuous, and $\mathbf{s}_\eta$ is the unique minimizer of $\mathcal{G}_n^\eta$.*
- **ii.** *If $\{\eta_i\}$ in $(0,1)$ is a sequence with $\eta_i \uparrow 1$ as $i \to \infty$, then $\mathbf{s}_{\eta_i} \rightharpoonup \mathbf{s}^*$ (along a subsequence) for some $\mathbf{s}^* \in H_0(\mathrm{div})$ and the latter is a minimizer of $\mathcal{G}_n$.*
- **iii.** *$(\mathbf{s}^*, P_{\mathcal{R}}(\mathbf{s}^*)) \in H_0(\mathrm{div}) \times \mathbf{L}^2(\Omega)$ is a minimizer of $\mathcal{E}_n^d$.*

**Algorithm 2** (Penalization with $\eta$ Parameter)

1: **Initialization.** Choose $\mathbf{t}_\eta^0 \in \mathcal{R} \subset \mathbf{L}^2(\Omega)$ arbitrary and set $k := 1$.
2: **Find**

$$\mathbf{s}_\eta^k = \underset{\mathbf{s}\in H_0(\mathrm{div})}{\arg\min} \frac{1}{2}|\mathrm{div}\mathbf{s} + f|_{L^2}^2 + \frac{q}{2}|\mathbf{s} - \eta\mathbf{t}_\eta^{k-1}|_{\mathbf{L}^2}^2.$$

3: **Find**

$$\mathbf{t}_\eta^k = \underset{\mathbf{t}\in\mathbf{L}^2(\Omega)}{\arg\min} \frac{q}{2}|\mathbf{s}_\eta^k - \mathbf{t}|_{\mathbf{L}^2}^2 + \delta_{\mathcal{R}}(\mathbf{t}).$$

4: Set $k := k + 1$ and return to step 2.

*Proof.* We start by proving **i**. Let $\mathbf{t} \in \mathbf{L}^2(\Omega)$ be fixed, and define $\mathcal{Q}(\mathbf{s}) = \frac{1}{2}|\mathrm{div}\mathbf{s} + f|_{L^2}^2 + \frac{q}{2}|\mathbf{s} - \eta\mathbf{t}|_{\mathbf{L}^2}^2$ for $\mathbf{s} \in H_0(\mathrm{div})$. Then, $\mathcal{Q}$ is clearly continuous and the inequality

$$\mathcal{Q}(\mathbf{s}) \geq \frac{1}{2}(|\mathrm{div}\mathbf{s}|_{L^2} - |f|_{L^2})^2 + \frac{q}{2}(|\mathbf{s}|_{\mathbf{L}^2} - \eta|\mathbf{t}|_{\mathbf{L}^2})^2,$$

implies that $\mathcal{Q}$ is coercive. Also, since the norms in $L^2(\Omega)$ and $\mathbf{L}^2(\Omega)$ are strictly convex and weakly lower semi-continuous $\mathbf{s} \mapsto \mathcal{Q}(\mathbf{s})$ is strictly convex and weakly lower semicontinuous in $H_0(\mathrm{div})$ and hence it admits a unique global minimizer. Thus, $\mathbf{s}_\eta^k$ is well-defined in step 2 of Algorithm 2 and we can write $\mathbf{s}_\eta^k = T(\eta\mathbf{t}_\eta^{k-1})$ (for $k \in \mathbb{N}$) where $T(\eta\cdot) : \mathbf{L}^2(\Omega) \to H_0(\mathrm{div})$. Since $\mathcal{R}$ is closed, convex and non-empty in $\mathbf{L}^2(\Omega)$, step 3 of Algorithm 2 is equivalent to the projection of $\mathbf{s}$ onto $\mathcal{R}$ and hence $\mathbf{t}_\eta^k$ is uniquely defined as $\mathbf{t}_\eta^k = P_{\mathcal{R}}(\mathbf{s}_\eta^k)$. Therefore, we can write $\mathbf{s}_\eta^k = T(\eta P_{\mathcal{R}}(\mathbf{s}_\eta^{k-1}))$.

Next, consider $|v|_q^2 := |\mathrm{div}\mathbf{s}|_{L^2}^2 + q|\mathbf{s}|_{\mathbf{L}^2}^2$ for $v \in H_0(\mathrm{div})$, which defines an equivalent norm to $|\cdot|_{H_0(\mathrm{div})}$. We now prove that $T(\eta P_{\mathcal{R}}(\cdot))$ is a contraction with respect to this norm. As the functional being minimized in step 2 of Algorithm 2 is differentible in $H_0(\mathrm{div})$, the first order optimality condition for $\mathbf{s}_i = T(\mathbf{t}_i)$ for $i = 1, 2$ reads

$$(\mathrm{div}\mathbf{s}_i + f, \mathrm{div}\mathbf{h}_i)_{L^2} + q(\mathbf{s}_i - \mathbf{t}_i, \mathbf{h}_i)_{\mathbf{L}^2} = 0, \quad \forall \mathbf{h}_i \in H_0(\mathrm{div}). \tag{3.9}$$

Taking $\mathbf{h}_1 = \mathbf{h}_2 = \mathbf{s}_2 - \mathbf{s}_1$ above, and subtracting the equality for $i = 2$ from the one for $i = 1$, we obtain

$$|\mathrm{div}(\mathbf{s}_2 - \mathbf{s}_1)|_{L^2}^2 + q|\mathbf{s}_2 - \mathbf{s}_1|_{\mathbf{L}^2}^2 = q(\mathbf{t}_2 - \mathbf{t}_1, \mathbf{s}_2 - \mathbf{s}_1)_{\mathbf{L}^2}.$$

This yields $|\delta\mathbf{s}|_q^2 \leq q|\delta\mathbf{t}|_{\mathbf{L}^2}|\delta\mathbf{s}|_{\mathbf{L}^2}$, with $\delta\mathbf{s} = \mathbf{s}_2 - \mathbf{s}_1$ and $\delta\mathbf{t} = \mathbf{t}_2 - \mathbf{t}_1$. This implies that $|\delta\mathbf{s}|_q \leq q^{1/2}|\delta\mathbf{t}|_{\mathbf{L}^2}$. Since $\mathbf{L}^2(\Omega)$ is a Hilbert space, we have $|P_{\mathcal{R}}(\mathbf{u}_2) - P_{\mathcal{R}}(\mathbf{u}_1)|_{\mathbf{L}^2} \leq |\mathbf{u}_2 - \mathbf{u}_1|_{\mathbf{L}^2}$ for all $\mathbf{u_1}, \mathbf{u_2} \in H_0(\mathrm{div}) \subset \mathbf{L}^2(\Omega)$. Then, for $\mathbf{t}_i = \eta P_{\mathcal{R}}(\mathbf{u}_i)$ we infer that $|\delta\mathbf{s}|_q \leq \eta q^{1/2}|\delta\mathbf{u}|_{\mathbf{L}^2} \leq \eta|\delta\mathbf{u}|_q$, i.e.,

$$|T(\eta P_{\mathcal{R}}(\mathbf{u}_2)) - T(\eta P_{\mathcal{R}}(\mathbf{u}_1))|_q \leq \eta|\mathbf{u}_2 - \mathbf{u}_1|_q. \tag{3.10}$$

Since $0 < \eta < 1$, by the Banach Contraction Principle, the sequence $\mathbf{s}_\eta^k = T(\eta P_{\mathcal{R}}(\mathbf{s}_\eta^{k-1}))$ converges strongly to $\mathbf{s}_\eta$ (in the $q$-norm and hence in the usual norm for $H_0(\mathrm{div})$, as well) which is the unique fixed point for $H_0(\mathrm{div}) \ni \mathbf{s} \mapsto T(\eta P_{\mathcal{R}}(\mathbf{s}))$. This implies that $\mathbf{s}_\eta$ is the unique minimizer of $H_0(\mathrm{div}) \ni \mathbf{s} \mapsto \mathcal{G}_n^\eta(\mathbf{s})$ in (3.8). In fact, if there were

other minimizers, then these minimizers would also be fixed points of $T(\eta P_{\mathcal{R}}(\cdot))$, which contradict the above argument.

Above, we have shown that $|\delta\mathbf{s}|_q \leq q^{1/2}|\delta\mathbf{t}|_{\mathbf{L}^2}$ for $\mathbf{s}_i = T(\mathbf{t}_i)$, $i = 1, 2$. Now, let $\eta_1, \eta_2 \in (0, 1)$. Hence there exist $\mathbf{s}_{\eta_i} \in H_0(\mathrm{div})$ such that $\mathbf{s}_{\eta_i} = T(\eta_i P_{\mathcal{R}}(\mathbf{s}_{\eta_i}))$. Since $|P_{\mathcal{R}}(\mathbf{s}_{\eta_i})|_{\mathbf{L}^2} \leq \alpha$ by the definition of $\mathcal{R}$ and because the projection map $P_{\mathcal{R}}$ is non-expansive, we have

$$|\mathbf{s}_{\eta_2} - \mathbf{s}_{\eta_1}|_q \leq q^{1/2}|\eta_2 P_{\mathcal{R}}(\mathbf{s}_{\eta_2}) - \eta_1 P_{\mathcal{R}}(\mathbf{s}_{\eta_1})|_{\mathbf{L}^2} \leq q^{1/2}(\eta_2|\mathbf{s}_{\eta_2} - \mathbf{s}_{\eta_1}|_{\mathbf{L}^2} + \alpha|\eta_2 - \eta_1|).$$

From this, it is straightforward to conclude

$$|\mathbf{s}_{\eta_2} - \mathbf{s}_{\eta_1}|_{\mathbf{L}^2} \leq \frac{\alpha}{1-\eta_2}|\eta_2 - \eta_1| \quad \text{and} \quad |\mathrm{div}(\mathbf{s}_{\eta_2} - \mathbf{s}_{\eta_1})|_{L^2} \leq \frac{\alpha q^{1/2}}{1-\eta_2}|\eta_2 - \eta_1|.$$

Hence, $\eta \mapsto \mathbf{s}_\eta$ is locally Lipschitz continuous on $(0, 1)$. This concludes the proof of **i**.

We now proceed with the proof of **ii**. Take a sequence $\{\eta_i\}$ in $(0, 1)$ such that $\eta_i \uparrow 1$ as $i \to \infty$ and consider the sequence $\{\mathbf{s}_{\eta_i}\}$ of fixed points $\mathbf{s}_{\eta_i} = T(\eta P_{\mathcal{R}}(\mathbf{s}_{\eta_i})) = \arg\min_{\mathbf{s}\in H_0(\mathrm{div})} \mathcal{G}_n^{\eta_i}(\mathbf{s})$. Then

$$\begin{aligned}\frac{1}{2}|f|_{L^2}^2 = \mathcal{G}_n^{\eta_i}(0) &\geq \min_{\mathbf{s}\in H_0(\mathrm{div})} \mathcal{G}_n^{\eta_i}(\mathbf{s}) = \mathcal{G}_n^{\eta_i}(\mathbf{s}_{\eta_i}) \\ &\geq \frac{1}{2}(|\mathrm{div}\mathbf{s}_{\eta_i}|_{L^2} - |f|_{L^2})^2 + \frac{q}{2}(|\mathbf{s}_{\eta_i}|_{\mathbf{L}^2} - \eta_i|P_{\mathcal{R}}(\mathbf{s}_{\eta_i})|_{\mathbf{L}^2})^2.\end{aligned}$$

Since $|P_{\mathcal{R}}(\mathbf{s}_{\eta_i})|_{\mathbf{L}^2} \leq \alpha$, the sequences $\{|\mathrm{div}\mathbf{s}_{\eta_i}|_{L^2}\}$ and $\{|\mathbf{s}_{\eta_i}|_{\mathbf{L}^2}\}$ are uniformly bounded. Hence, $\{\mathbf{s}_{\eta_i}\}$ is bounded in $H_0(\mathrm{div})$, and since the latter is a reflexive space, there exists a subsequence of $\{\mathbf{s}_{\eta_i}\}$ (again denoted by $\{\mathbf{s}_{\eta_i}\}$) such that $\mathbf{s}_{\eta_i} \rightharpoonup \mathbf{s}^*$ for some $\mathbf{s}^* \in H_0(\mathrm{div})$ as $i \to \infty$.

We now prove that $\mathbf{s}^*$ is a minimizer of $\mathbf{s} \mapsto \mathcal{G}_n(\mathbf{s})$. For this purpose, we note that the sequence $\{P_{\mathcal{R}}(\mathbf{s}_{\eta_i})\} \subset \mathcal{R}$ is bounded in $\mathbf{L}^2(\Omega)$. Hence, there exists a subsequence of $\{P_{\mathcal{R}}(\mathbf{s}_{\eta_i})\}$ (also denoted by $\{P_{\mathcal{R}}(\mathbf{s}_{\eta_i})\}$) for which $P_{\mathcal{R}}(\mathbf{s}_{\eta_i}) \rightharpoonup z$ for some $z \in \mathcal{R} \subset \mathbf{L}^2(\Omega)$. Since $\mathbf{s}_{\eta_i} \rightharpoonup \mathbf{s}^*$, we have $(\mathbf{s}_{\eta_i} - \eta_i P_{\mathcal{R}}(\mathbf{s}_{\eta_i})) \rightharpoonup (\mathbf{s}^* - z)$ in $\mathbf{L}^2(\Omega)$ as $i \to \infty$. Here we use the fact that $H_0(\mathrm{div}) \hookrightarrow \mathbf{L}^2(\Omega)$ is a dense and continuous embedding, and so is the embedding $\mathbf{L}^2(\Omega)^* \equiv \mathbf{L}^2(\Omega) \hookrightarrow H_0(\mathrm{div})^*$. Hence if $\{z_n\} \subset H_0(\mathrm{div})$ such that $(l, z_n)_{H_0(\mathrm{div})^*, H_0(\mathrm{div})} \to (l, z)_{H_0(\mathrm{div})^*, H_0(\mathrm{div})}$ for all $l \in H_0(\mathrm{div})^*$, the same holds if $l \in \mathbf{L}^2(\Omega)$. Thus, since $z \in \mathcal{R}$, by the weak lower semicontinuity of the norm we have

$$|\mathbf{s}^* - P_{\mathcal{R}}(\mathbf{s}^*)|_{\mathbf{L}^2} \leq |\mathbf{s}^* - z|_{\mathbf{L}^2} \leq \varliminf_{i\to\infty} |\mathbf{s}_{\eta_i} - \eta_i P_{\mathcal{R}}(\mathbf{s}_{\eta_i})|_{\mathbf{L}^2},$$

where we utilize the minimal distance property of the projection $P_{\mathcal{R}}$. Let $\mathbf{s} \in H_0(\mathrm{div})$

be arbitrary. Then

$$\begin{aligned}\frac{1}{2}|\mathrm{div}\mathbf{s}^* + f|_{L^2}^2 + \frac{q_n}{2}|\mathbf{s}^* - P_{\mathcal{R}}(\mathbf{s}^*)|_{\mathbf{L}^2}^2 &\leq \frac{1}{2}|\mathrm{div}\mathbf{s}^* + f|_{L^2}^2 + \frac{q_n}{2}|\mathbf{s}^* - z|_{\mathbf{L}^2}^2 \\ &\leq \left(\varliminf_{i\to\infty} \frac{1}{2}|\mathrm{div}\mathbf{s}_{\eta_i} + f|_{L^2}^2\right) + \left(\varliminf_{i\to\infty} \frac{q_n}{2}|\mathbf{s}_{\eta_i} - \eta_i P_{\mathcal{R}}(\mathbf{s}_{\eta_i})|_{\mathbf{L}^2}^2\right) \\ &\leq \varliminf_{i\to\infty} \left(\frac{1}{2}|\mathrm{div}\mathbf{s}_{\eta_i} + f|_{L^2}^2 + \frac{q_n}{2}|\mathbf{s}_{\eta_i} - \eta_i P_{\mathcal{R}}(\mathbf{s}_{\eta_i})|_{\mathbf{L}^2}^2\right) \\ &= \varliminf_{i\to\infty} \mathcal{G}_n^{\eta_i}(\mathbf{s}_{\eta_i}) \leq \varliminf_{i\to\infty} \mathcal{G}_n^{\eta_i}(\mathbf{s}) \\ &= \varliminf_{i\to\infty} \left(\frac{1}{2}|\mathrm{div}\mathbf{s} + f|_{L^2}^2 + \frac{q_n}{2}|\mathbf{s} - \eta_i P_{\mathcal{R}}(\mathbf{s})|_{\mathbf{L}^2}^2\right) \\ &= \frac{1}{2}|\mathrm{div}\mathbf{s} + f|_{L^2}^2 + \frac{q_n}{2}|\mathbf{s} - P_{\mathcal{R}}(\mathbf{s})|_{\mathbf{L}^2}^2,\end{aligned}$$

i.e., $\mathcal{G}_n(\mathbf{s}^*) = \inf_{\mathbf{s}\in H_0(\mathrm{div})} \mathcal{G}_n(\mathbf{s})$.

Finally, we consider **iii**. Let $(\mathbf{s},\mathbf{t}) \in H_0(\mathrm{div}) \times \mathbf{L}^2(\Omega)$ be arbitrary. Since we have proven that $\mathbf{s}^*$ is a minimizer of $\mathbf{s} \mapsto \mathcal{G}_n(\mathbf{s})$, by the minimum distance property of $P_{\mathcal{R}}$, we get

$$\begin{aligned}\mathcal{E}_n^d(\mathbf{s}^*, P_{\mathcal{R}}(\mathbf{s}^*)) = \mathcal{G}_n(\mathbf{s}^*) \leq \mathcal{G}_n(\mathbf{s}) &= \frac{1}{2}|\mathrm{div}\mathbf{s} + f|_{L^2}^2 + \frac{q_n}{2}|\mathbf{s} - P_{\mathcal{R}}(\mathbf{s})|_{\mathbf{L}^2}^2 \\ &\leq \frac{1}{2}|\mathrm{div}\mathbf{s} + f|_{L^2}^2 + \frac{q_n}{2}|\mathbf{s} - \mathbf{t}|_{\mathbf{L}^2}^2 + \delta_{\mathcal{R}}(\mathbf{t}) \\ &= \mathcal{E}_n^d(\mathbf{s},\mathbf{t}).\end{aligned}$$

Henceforth, taking the infimum over $(\mathbf{s},\mathbf{t}) \in H_0(\mathrm{div})\times\mathbf{L}^2(\Omega)$, we obtain $\mathcal{E}_n^d(\mathbf{s}^*, P_{\mathcal{R}}(\mathbf{s}^*)) \leq \inf_{(\mathbf{s},\mathbf{t})\in H_0(\mathrm{div})\times\mathbf{L}^2(\Omega)} \mathcal{E}_n^d(\mathbf{s},\mathbf{t})$, i.e., $(\mathbf{s}^*, P_{\mathcal{R}}(\mathbf{s}^*))$ is a minimizer of $\mathcal{E}_n^d$. □

**3.2. Augmented Lagrangian Method.** In order to avoid a limiting process of the penalty parameter $q_n$, we prove that an approach based on the augmented Lagrangian method is suitable for the problem in this respect. For this purpose, denote $Y = H_0(\mathrm{div}) \times \mathbf{L}^2(\Omega)$. Then, we consider the following family of problems with regularization parameter $\epsilon \geq 0$:

$$\text{(3.11a)} \qquad \text{Minimize } \mathcal{J}_d^\epsilon(\mathbf{s}) := \frac{1}{2}|\mathrm{div}\mathbf{s} + f|_{L^2}^2 + \frac{\epsilon}{2}|\mathbf{s}|_{\mathbf{L}^2}^2 \quad \text{over } (\mathbf{s},\mathbf{t}) \in Y,$$

$$\text{(3.11b)} \qquad \text{s.t.} \quad \mathbf{t} \in \mathcal{R} \text{ and } g(\mathbf{s},\mathbf{t}) := \mathbf{s} - \mathbf{t} = 0,$$

with $\mathcal{J}_d^\epsilon : H_0(\mathrm{div}) \to \mathbb{R}$ and $g : Y \to \mathbf{L}^2(\Omega)$. The objective $\mathcal{J}_d^\epsilon$ is coercive, convex (strictly if $\epsilon > 0$) and continuous (and hence lower semicontinuous) and $\mathcal{R}$ is closed, convex and non-empty. Therefore there exists a solution $\mathbf{s}^*$ (which is unique if $\epsilon > 0$) that solves the minimization problem (3.11) and $\mathbf{s}^* \in \mathcal{R}$.

We consider the Lagrangian $\mathcal{L}^d : Y \times \mathbf{L}^2(\Omega) \to \mathbb{R} \cup \{+\infty\}$ and the associated augmented Lagrangian $\mathcal{L}_{\mathrm{Aug}}^d : Y \times \mathbf{L}^2(\Omega) \times \mathbb{R}^+ \to \mathbb{R} \cup \{+\infty\}$ defined as

$$\text{(3.12)} \qquad \mathcal{L}^d(\mathbf{s},\mathbf{t},\boldsymbol{\lambda}) := \frac{1}{2}|\mathrm{div}\mathbf{s} + f|_{L^2}^2 + \frac{\epsilon}{2}|\mathbf{s}|_{\mathbf{L}^2}^2 + \delta_{\mathcal{R}}(\mathbf{t}) + (\boldsymbol{\lambda}, \mathbf{s} - \mathbf{t})_{\mathbf{L}^2},$$

$$\text{(3.13)} \qquad \mathcal{L}_{\mathrm{Aug}}^d(\mathbf{s},\mathbf{t},\boldsymbol{\lambda},q) := \frac{1}{2}|\mathrm{div}\mathbf{s} + f|_{L^2}^2 + \frac{\epsilon}{2}|\mathbf{s}|_{\mathbf{L}^2}^2 + \delta_{\mathcal{R}}(\mathbf{t}) + (\boldsymbol{\lambda}, \mathbf{s} - \mathbf{t})_{\mathbf{L}^2} + \frac{q}{2}|\mathbf{s} - \mathbf{t}|_{L^2}^2.$$

Since $g$ is Fréchet differentiable and $Dg(\mathbf{s},\mathbf{t}) \in \mathscr{L}(Y, \mathbf{L}^2(\Omega))$, given by $Dg(\mathbf{s},\mathbf{t})(\mathbf{h}_1,\mathbf{h}_2) = \mathbf{h}_1 - \mathbf{h}_2$, we observe that

$$0 \in \operatorname{int}\{Dg(\mathbf{s},\mathbf{t})(H_0(\mathrm{div}) \times \mathcal{R} - (\mathbf{s},\mathbf{t})) + g(\mathbf{s},\mathbf{t})\} = \operatorname{int}\{\mathbf{r}_1 - \mathbf{r}_2 : \mathbf{r}_1 \in H_0(\mathrm{div}), \mathbf{r}_2 \in \mathcal{R}\},$$

where the interior is taken in $\mathbf{L}^2(\Omega)$. Then, by standard surjectivity techniques (see [18, 29]) there exists a Lagrange multiplier $\boldsymbol{\lambda}^* \in \mathbf{L}^2(\Omega)$ such that $\langle \boldsymbol{\lambda}^*, \mathbf{s}^* - \mathbf{t}^* \rangle_{\mathbf{L}^2} = 0$ and

$$D\mathcal{J}_d^\epsilon(\mathbf{s}^*) + \boldsymbol{\lambda}^* \circ Dg(\mathbf{s}^*,\mathbf{t}^*) \in -\mathcal{R}(\mathbf{s}^*,\mathbf{t}^*)^+, \tag{3.14}$$

where $\mathcal{R}(\mathbf{s}^*,\mathbf{t}^*)^+$ is the polar cone of the conical hull of $\mathcal{R} \setminus (\mathbf{s}^*,\mathbf{t}^*)$, i.e.,

$$-\mathcal{R}(\mathbf{s}^*,\mathbf{t}^*)^+ = \{F \in Y^* : (F, (\mathbf{s}^*,\mathbf{t}^*))_{Y^*,Y} \le (F, (\mathbf{r}_1,\mathbf{r}_2))_{Y^*,Y}, \forall \mathbf{r}_1 \in H_0(\mathrm{div}), \mathbf{r}_2 \in \mathcal{R}\}.$$

Hence (3.14) is equivalent to

$$\begin{aligned}(\mathrm{div}\mathbf{s}^* + f, \mathrm{div}\mathbf{s}^*)_{L^2} + \epsilon(\mathbf{s}^*,\mathbf{s}^*)_{\mathbf{L}^2} + (\boldsymbol{\lambda}^*, \mathbf{s}^* - \mathbf{t}^*)_{\mathbf{L}^2} \le \\ (\mathrm{div}\mathbf{s}^* + f, \mathrm{div}\mathbf{r}_1)_{L^2} + \epsilon(\mathbf{s}^*,\mathbf{r}_1)_{\mathbf{L}^2} + (\boldsymbol{\lambda}^*, \mathbf{r}_1 - \mathbf{r}_2)_{\mathbf{L}^2}, \quad \forall \mathbf{r}_1 \in H_0(\mathrm{div}), \mathbf{r}_2 \in \mathcal{R}.\end{aligned}$$

Here we have used $D\mathcal{J}_d^\epsilon(\mathbf{s})(\mathbf{h}_1,\mathbf{h}_2) = (\mathrm{div}\mathbf{s} + f, \mathrm{div}\mathbf{h}_1)_{L^2} + \epsilon(\mathbf{s},\mathbf{h}_1)_{\mathbf{L}^2}$ for all $(\mathbf{s},\mathbf{t}), (\mathbf{h}_1,\mathbf{h}_2) \in Y$. This implies that

$$(\boldsymbol{\lambda}^*, \mathbf{s}^* - \mathbf{t}^*)_{\mathbf{L}^2} \le (\boldsymbol{\lambda}^*, \mathbf{r}_1 - \mathbf{r}_2)_{\mathbf{L}^2} + D\mathcal{J}_d^\epsilon(\mathbf{s}^*)(\mathbf{r}_1 - \mathbf{s}^*) \quad \forall \mathbf{r}_1 \in H_0(\mathrm{div}), \mathbf{r}_2 \in \mathcal{R}. \tag{3.15}$$

THEOREM 3.3. *Let $(\mathbf{s}^*,\mathbf{t}^*) \in Y$ be a solution (the unique one in case $\epsilon > 0$) to (3.11), and let $\boldsymbol{\lambda}^*$ be the associated Lagrange multiplier. Then, for $q > 0$, $(\mathbf{s}^*,\mathbf{t}^*)$ is a global minimizer (unique in the case $\epsilon > 0$) of the map*

$$Y \ni (\mathbf{s},\mathbf{t}) \mapsto \mathcal{L}_{\mathrm{Aug}}^d(\mathbf{s},\mathbf{t},\boldsymbol{\lambda}^*,q).$$

*Proof.* It is straightforward to observe that, for $\mathbf{s} \in H_0(\mathrm{div})$, $D^2\mathcal{J}_d^\epsilon(\mathbf{s}) \in \mathscr{L}(H_0(\mathrm{div}) \times H_0(\mathrm{div}), \mathbb{R})$ is given by

$$D^2\mathcal{J}_d^\epsilon(\mathbf{s})(\mathbf{h}_1,\mathbf{h}_2) = (\mathrm{div}\mathbf{h}_2, \mathrm{div}\mathbf{h}_1)_{L^2} + \epsilon(\mathbf{h}_2,\mathbf{h}_1)_{\mathbf{L}^2}, \qquad \forall \mathbf{h}_1,\mathbf{h}_2 \in H_0(\mathrm{div}),$$

from where we observe $D^3\mathcal{J}_d^\epsilon(\mathbf{s}) = 0$. Assuming that $0 < \epsilon < 1$, we have $D^2\mathcal{J}_d^\epsilon(\mathbf{s})(\mathbf{h},\mathbf{h}) = |\mathrm{div}\mathbf{h}|_{L^2}^2 + \epsilon|\mathbf{h}|_{\mathbf{L}^2}^2 \ge \epsilon|\mathbf{h}|_{H_0(\mathrm{div})}^2$. We also have the following representation based on a Taylor series expansion:

$$\mathcal{J}_d^\epsilon(\mathbf{s}+\mathbf{h}) = \mathcal{J}_d^\epsilon(\mathbf{s}) + D\mathcal{J}_d^\epsilon(\mathbf{s})(\mathbf{h}) + \frac{1}{2}D^2\mathcal{J}_d^\epsilon(\mathbf{s})(\mathbf{h},\mathbf{h}), \qquad \forall \mathbf{h} \in H_0(\mathrm{div}).$$

Since $\mathcal{L}_{\mathrm{Aug}}^d(\mathbf{s},\mathbf{t},\boldsymbol{\lambda}^*,q) = +\infty$ if $\mathbf{t} \notin \mathcal{R}$, it is enough to consider $(\mathbf{s},\mathbf{t}) \in H_0(\mathrm{div}) \times \mathcal{R}$. Since $(\mathbf{s}^*,\mathbf{t}^*) \in Y$ is a solution to (3.11), we have that $|\mathbf{s}^* - \mathbf{t}^*|_{\mathbf{L}^2} = 0$. Then, by the previous paragraph and (3.15), we have the following chain of inequalities:

$$\begin{aligned}\mathcal{L}_{\mathrm{Aug}}^d(\mathbf{s}^*,\mathbf{t}^*,\boldsymbol{\lambda}^*,q) &= \mathcal{J}_d^\epsilon(\mathbf{s}^*) + \delta_{\mathcal{R}}(\mathbf{t}^*) + (\boldsymbol{\lambda}^*, \mathbf{s}^* - \mathbf{t}^*)_{\mathbf{L}^2} \\ &\le \mathcal{J}_d^\epsilon(\mathbf{s}^*) + \delta_{\mathcal{R}}(\mathbf{t}^*) + (\boldsymbol{\lambda}^*, \mathbf{s} - \mathbf{t})_{\mathbf{L}^2} + D\mathcal{J}_d^\epsilon(\mathbf{s}^*)(\mathbf{s} - \mathbf{s}^*) \\ &= \mathcal{J}_d^\epsilon(\mathbf{s}^*) + \delta_{\mathcal{R}}(\mathbf{t}) + (\boldsymbol{\lambda}^*, \mathbf{s} - \mathbf{t})_{\mathbf{L}^2} + D\mathcal{J}_d^\epsilon(\mathbf{s}^*)(\mathbf{s} - \mathbf{s}^*) \\ &= \mathcal{J}_d^\epsilon(\mathbf{s}) - \frac{1}{2}D^2\mathcal{J}_d^\epsilon(\mathbf{s}^*)(\mathbf{s} - \mathbf{s}^*, \mathbf{s} - \mathbf{s}^*) + \delta_{\mathcal{R}}(\mathbf{t}) + (\boldsymbol{\lambda}^*, \mathbf{s} - \mathbf{t})_{\mathbf{L}^2} \\ &= \mathcal{L}_{\mathrm{Aug}}^d(\mathbf{s},\mathbf{t},\boldsymbol{\lambda}^*,q) - \frac{1}{2}D^2\mathcal{J}_d^\epsilon(\mathbf{s}^*)(\mathbf{s} - \mathbf{s}^*, \mathbf{s} - \mathbf{s}^*) - \frac{q}{2}|\mathbf{s} - \mathbf{t}|_{\mathbf{L}^2}^2.\end{aligned}$$

Then, for $\epsilon > 0$, we have

$$\mathcal{L}^d_{\mathrm{Aug}}(\mathbf{s}^*, \mathbf{t}^*, \boldsymbol{\lambda}^*, q) \leq \mathcal{L}^d_{\mathrm{Aug}}(\mathbf{s}, \mathbf{t}, \boldsymbol{\lambda}^*, q) - \frac{\epsilon}{2}|\mathbf{s} - \mathbf{s}^*|^2_{H_0(\mathrm{div})} - \frac{q}{2}|\mathbf{s} - \mathbf{t}|^2_{\mathbf{L}^2},$$

and for $\epsilon = 0$,

$$\mathcal{L}^d_{\mathrm{Aug}}(\mathbf{s}^*, \mathbf{t}^*, \boldsymbol{\lambda}^*, q) \leq \mathcal{L}^d_{\mathrm{Aug}}(\mathbf{s}, \mathbf{t}, \boldsymbol{\lambda}^*, q) - \frac{1}{2}|\mathrm{div}(\mathbf{s} - \mathbf{s}^*)|^2_{L^2} - \frac{q}{2}|\mathbf{s} - \mathbf{t}|^2_{\mathbf{L}^2}.$$

□

**3.2.1. The Discrete Penalized Problem.** In this subsection, the advantages of the penalty method with variable splitting in the Fenchel pre-dual formulation are discussed in finite dimensions.

For a given $N \times N$ image $f \in \mathbb{R}^{N^2}$, we denote by $\Omega_h = \{1, \ldots, N\} \times \{1, \ldots, N\}$ the discretization of $\Omega = (0,1) \times (0,1)$ with mesh size $h = \frac{1}{N}$. The discrete optimization problem associated to (3.5) is as follows:

$$\begin{aligned} &\text{Minimize } \mathcal{E}^d_{n,h}(\mathbf{s}, \mathbf{t}) \quad \text{over } (\mathbf{s}, \mathbf{t}) \in Y_h = \mathbb{R}^{2N^2} \times \mathbb{R}^{2N^2}, \\ &\mathcal{E}^d_{n,h}(\mathbf{s}, \mathbf{t}) := h^2 \sum_{(i,j) \in \Omega_h} \frac{1}{2}|(\mathrm{div}_h \mathbf{s})_{i,j} + f_{i,j}|^2 + \frac{q_n}{2}|\mathbf{s}_{i,j} - \mathbf{t}_{i,j}|^2 + \delta_{\mathcal{R}_h}(\mathbf{t}), \end{aligned} \tag{3.16}$$

where $\mathcal{R}_h = \{\mathbf{t} \in \mathbb{R}^{2N^2} \mid |\mathbf{t}_{i,j}| \leq \alpha,\ (i,j) \in \Omega_h\}$, and the discrete indicator function is defined by

$$\delta_{\mathcal{R}_h}(\mathbf{t}) = \begin{cases} 0 & \mathbf{t} \in \mathcal{R}_h, \\ +\infty & \text{otherwise.} \end{cases} \tag{3.17}$$

We use an alternating minimization algorithm, Algorithm 3, to generate a sequence $\{(\mathbf{s}^k_{n,h}, \mathbf{t}^k_{n,h})\}_{k \in \mathbb{N}}$ with a fixed positive penalty parameter $q_n$ and $0 < \eta < 1$.

**Algorithm 3** (Discrete Penalization with $\eta$ Parameter)

1: **Initialization.** Choose $\mathbf{t}^0_{n,h} \in \mathcal{R}_h$ arbitrary and set $k := 1$.
2: **Compute**

$$\mathbf{s}^k_{n,h} \in \arg\min_{\mathbf{s}} \sum_{(i,j) \in \Omega_h} \frac{1}{2}|(\mathrm{div}_h \mathbf{s})_{i,j} + f_{i,j}|^2 + \frac{q_n}{2}|\mathbf{s}_{i,j} - \eta(\mathbf{t}^{k-1}_{n,h})_{i,j}|^2.$$

3: **Compute**

$$\mathbf{t}^k_{n,h} \in \arg\min_{\mathbf{t}} \sum_{(i,j) \in \Omega_h} \frac{q_n}{2}|(\mathbf{s}^k_{n,h})_{i,j} - \mathbf{t}_{i,j}|^2 + \delta_{\mathcal{R}_h}(\mathbf{t}).$$

4: **Check stopping criteria.** If suitable stopping criteria are met, $(\mathbf{s}^*_{n,h}, \mathbf{t}^*_{n,h}) = (\mathbf{s}^k_{n,h}, \mathbf{t}^k_{n,h})$; otherwise set $k := k + 1$ are return to step 2.

A few words on Algorithm 3 are in order. The introduction of the variable $\mathbf{t}$ in the functional $\mathcal{E}^d_n(\mathbf{s}, \mathbf{t})$ in (3.5) helps to handle the pointwise inequality constraint

in the numerical implementation. The alternating direction algorithm with the variable $\mathbf{t}$ divides the minimization problems for $\mathcal{E}^d_{n,h}(\mathbf{s},\mathbf{t})$ in Algorithm 3 into two parts. Each subproblem has a unique solution and their respective numerical implementation is rather straightforward. In fact, the first-order optimality condition of the $\mathbf{s}$-subproblem reduces to a linear elliptic partial differential equation of the second order, and a soft-thresholding method gives an explicit solution for the $\mathbf{t}$-subproblem.

For a fixed $q_n$, suitable stopping criteria in step 4 of Algorithm 3 relate to the norm of the residual of the first-order optimality conditions dropping below a user-specified tolerance. A soft-thresholding technique provides an explicit formula for $\mathbf{t}^k_{n,h}$ in step 3, which satisfies the first-order condition of the $\mathbf{t}$-subproblem exactly. Thus, it is enough to check the residual of the first-order condition of the $\mathbf{s}$-subproblem. For this purpose, we compute

$$\mathbf{R}^k_{n,h} := -\nabla_h \left(\mathrm{div}_h \mathbf{s}^k_{n,h} + f\right) + q_n \left(\mathbf{s}^k_{n,h} - \eta \mathbf{t}^k_{n,h}\right), \tag{3.18}$$

and $\tilde{\mathbf{R}}^k_{n,h}$ such that $-\Delta_h \tilde{\mathbf{R}}^k_{n,h} = \mathbf{R}^k_{n,h}$ with homogeneous Dirichlet boundary conditions on $\partial\Omega_h$, where $\Delta_h$ denotes the discrete Laplacian on the underlying mesh. Then, the discrete $L^2(\Omega)$-norm of $\nabla_h \tilde{\mathbf{R}}^k_{n,h}$ provides the discrete $H^{-1}(\Omega)$-norm of $\mathbf{R}^k_{n,h}$.

The value of $\mathbf{s}^*_{n,h}$ in step 4 of Algorithm 3 is, in virtue of the above paragraph, $\mathbf{s}^k_{n,h}$ for the smallest $k$ that satisfies

$$|\nabla_h \tilde{\mathbf{R}}^k_{n,h}|_{\mathbf{L}^2} \leq \epsilon_d, \tag{3.19}$$

where $\epsilon_d > 0$ is some prescribed tolerance. The aforementioned index $k > 0$ is the number of iterations of the algorithm and it is denoted as $K_{n,h}$, as it depends on the penalty parameter $r_n$ and the mesh size $h > 0$. Starting with $q_0 > 0$, and increasing the penalty parameter up to $q_n$, the total number of iterations is the sum of the iterations corresponding to each penalty parameter, i.e.,

$$K_h := \sum_{i=0}^{n} K_{i,h}. \tag{3.20}$$

Finally, the approximated solution of the discrete TV-problem is determined as

$$u^*_{n,h} = \mathrm{div}_h \mathbf{s}^*_{n,h} + f. \tag{3.21}$$

We use the same continuation scheme in [26] to increase the penalty parameter, i.e., $q_{n+1} = 2q_n$.

We also would like to emphasize the fact that our goal here is not to display the best possible reconstruction result, i.e., selecting optimal regularization parameters, but rather to focus on the algorithm and its behavior.

We start our numerical study by showing that the practical behavior of $\eta$ in (3) is consistent with Theorem 3.2. For this purpose, we use the image shown in Figure 3.1(a) which contains white Gaussian noise with zero mean and a standard deviation equal to 30. The parameters used in our algorithm are $\alpha = 0.2$, $\epsilon_d = 10^{-6}$ and the reconstruction is provided in Figure 3.1(b). Starting with a penalty parameter $q_0 = 2^{-5}$, we numerically compute $u^*_{n,h}$ for $n \in \{0, 1, \ldots, 24\}$ with $h = 1/128$. Since $u^*_{n,h}$ and $K_h$ depend on $\eta$, we stop our computations at $q_{25} = 2^{20}$ for all $\eta$-values and denote these as $u_\eta$ and $K_\eta$, respectively. In order to measure more detailed features when $\eta$ approaches 1, we choose $\eta_m$ according to

$$\eta_m = \sum_{i=1}^{m} 9 \cdot 10^{-i}. \tag{3.22}$$

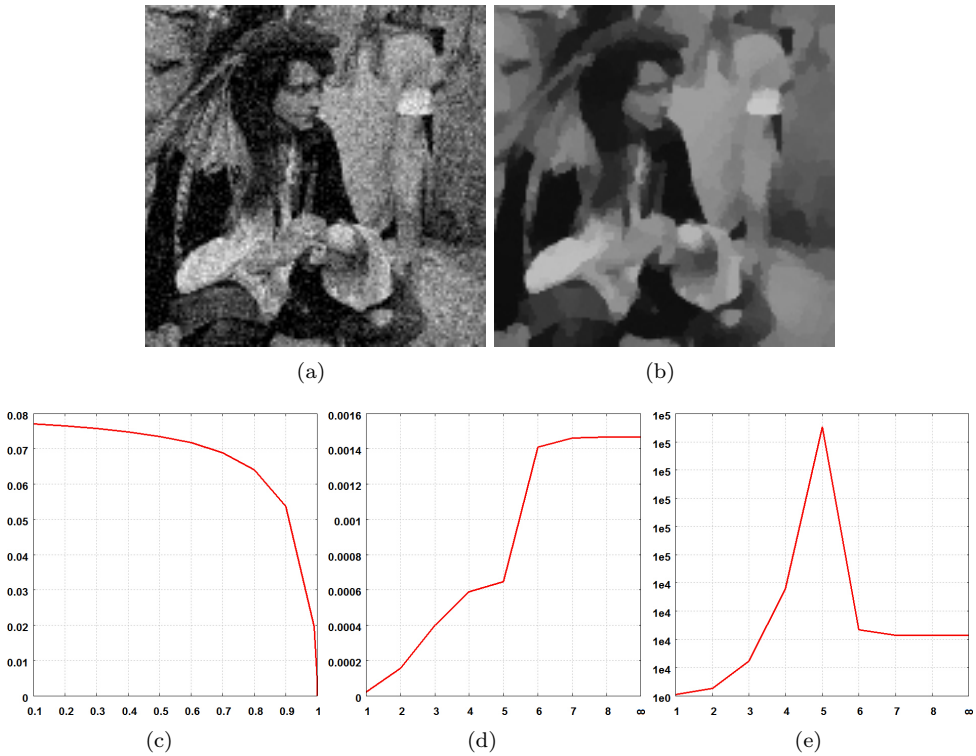


Fig. 3.1: In figures (a) and (b) we depict the test image with white Gaussian noise of zero mean and standard deviation equal to 30 and its reconstruction with $\alpha = 0.2$, respectively. In figure (c) we observe the behavior of the map $(0.1, 1) \ni \eta \mapsto |u_\eta - u_{\eta_\infty}|_{L^2}$, where $\eta_\infty = \eta_9 = 1 - 10^{-10}$. The $x$-axis in figures 3.1(d), 3.1(e) indicates the value $m$ in (3.22). In figure 3.1(d), we observe $m \mapsto |u_{\eta_m} - u_{\eta_m - c}|_{L^2}$, where $c = 10^{-3}$, and in Figure 3.1(e), the map $m \mapsto K_{\eta_m}$ (the total number of iterations associated with the parameter $\eta_m$) is shown.

Figure 3.1(c) shows the behavior of $|u_\eta - u_{\eta_\infty}|_{L^2}$ with respect to $\eta \in [0.1, 1)$, where $\eta_\infty$ denotes the maximum value used for $\eta$ which, in this case, is $\eta_9 = 1 - 10^{-10}$. As we are in finite dimensions upon discretization, convergence of $u_\eta$ in the discrete $L^2(\Omega)$-norm of the approximated solution to the TV-problem in (3.21) is observed when $\eta \to 1$. This behavior is guaranteed by Theorem 3.2(**ii.**) considered in finite dimensions. Local Lipschitz behavior of $\eta \mapsto u_\eta$ is observed for $\eta < 1$ and a non-Lipschitz behavior appears at $\eta = 1$, as expected by Theorem 3.2(**i.**).

Figure 3.1(d) shows the behavior of $m \mapsto |u_{\eta_m} - u_{\eta_\infty - c}|_{L^2}$ with respect to $m$ as in (3.22) and with $c = 10^{-3}$. This is consistent with the non-Lipschitz behavior of $\eta \mapsto u_\eta$ at $\eta = 1$ expected from Theorem 3.2(**i**). The total number of iterations $K_{\eta_m}$ with respect to $m$ as in (3.22) is shown in Figure 3.1(e). The behavior of the map $m \mapsto K_{\eta_m}$ appears to contain two distinct features that are explained by the contraction of the map $\mathbf{s} \mapsto T(\eta P_{\mathcal{R}}(\mathbf{s}))$, as noted in the proof of Theorem 3.2, and the fact we are working in finite dimensions upon discretization. In fact, as noted before, step 2 of Algorithm 2 is equivalent to $\mathbf{s}_\eta^k = T(\eta P_{\mathcal{R}}(\mathbf{s}_\eta^{k-1}))$. This iteration is at least

linearly convergent since $\mathbf{s} \mapsto T(\eta P_{\mathcal{R}}(\mathbf{s}))$ is a contraction in the $q$-norm for $H_0(\mathrm{div})$, as observed in (3.10). For this purpose, recall that the $q$-norm equivalent to the usual norm in $H_0(\mathrm{div})$. Since the Lipschitz constant is equal to $\eta$, it is expected that the increase of $\eta$ increases the number of iterations $K_\eta$ necessary to satisfy the small residual condition (3.19). This is indeed observed in Figure 3.1(e) for $1 \leq m \leq 5$. In infinite dimensions one would expect that this behavior continues for $m > 5$. In finite dimensions, the weak convergence in Theorem 3.2(**ii.**) becomes strong convergence in the discrete $L^2(\Omega)$-norm, which appears to take place for $m > 5$. This is the reason for the stabilization of the number of iterations necessary for the termination of the algorithm.

It should be noted that the $L^2$-penalty term associated to the constraint $\mathbf{s} = \mathbf{t}$ in (3.5) does not increase the regularity of the solution as it happens with the penalty of the constraint $\mathbf{p} = \nabla u$ in (2.2). This enables the restoration of discontinuous features in images, as motivated by the total variation regularization.

**3.2.2. The Discrete Augmented Lagrangian .** The discrete augmented Lagrangian associated with (3.13) is given by

$$\mathcal{L}^d_{q,h}(\mathbf{s},\mathbf{t};\boldsymbol{\mu}) := h^2 \sum_{(i,j)\in\Omega_h} \frac{1}{2}|(\mathrm{div}_h\mathbf{s})_{i,j} + f_{i,j}|^2 + \frac{q}{2}|\mathbf{s}_{i,j} - \mathbf{t}_{i,j}|^2 + \boldsymbol{\mu}_{i,j}\cdot(\mathbf{s}_{i,j} - \mathbf{t}_{i,j}) + \delta_{\mathcal{R}_h}(\mathbf{t}). \tag{3.23}$$

For a given positive penalty parameter $q \geq 0$ we use an alternating direction minimization algorithm to generate a sequence $\{(\mathbf{s}^k_{q,h}, \mathbf{t}^k_{q,h}, \boldsymbol{\mu}^k_{q,h})\}_{k\in\mathbb{N}}$ by Algorithm 4; see [20, 25] for details.

**Algorithm 4** (Discrete Pre-dual Augmented Lagrangian)

1: **Initialization.** Choose $(\mathbf{t}^0_{n,h}, \boldsymbol{\mu}^0_{n,h})$ and set $k := 1$.
2: **Compute**

$$\mathbf{s}^k_{q,h} \in \arg\min_{\mathbf{s}} \sum_{(i,j)\in\Omega_h} \frac{1}{2}|(\mathrm{div}_h\mathbf{s})_{i,j} + f_{i,j}|^2 + \frac{q}{2}|\mathbf{s}_{i,j} - (\mathbf{t}^{k-1}_{q,h})_{i,j}|^2 + \boldsymbol{\mu}^{k-1}_{i,j}\cdot\mathbf{s}_{i,j}.$$

3: **Compute**

$$\mathbf{t}^k_{q,h} \in \arg\min_{\mathbf{t}} \sum_{(i,j)\in\Omega_h} \frac{q}{2}|(\mathbf{s}^k_{q,h})_{i,j} - \mathbf{t}_{i,j}|^2 - \boldsymbol{\mu}^{k-1}_{i,j}\cdot\mathbf{t}_{i,j} + \delta_{\mathcal{R}_h}(\mathbf{t}).$$

4: **Set**

$$\left(\boldsymbol{\mu}^k_{q,h}\right)_{i,j} := \left(\boldsymbol{\mu}^{k-1}_{q,h}\right)_{i,j} + q\left(\left(\mathbf{s}^k_{q,h}\right)_{i,j} - \left(\mathbf{t}^k_{q,h}\right)_{i,j}\right), \quad (i,j)\in\Omega_h.$$

5: **Check stopping criteria.** If suitable stopping criteria are met, $(\mathbf{s}^*_{n,h}, \mathbf{t}^*_{n,h}, \boldsymbol{\mu}^*_{n,h}) := (\mathbf{s}^k_{n,h}, \mathbf{t}^k_{n,h}, \boldsymbol{\mu}^k_{n,h})$; otherwise set $k := k+1$ are return to step 2.

For a fixed $q_n$, as stated for previous algorithms, suitable stopping criteria in step 5 of Algorithm 4 are based on the norm of the residuals of the first-order optimality conditions dropping below a user-specified tolerance. As observed before, a soft-thresholding technique gives an explicit formula for $\mathbf{t}^k_{q,h}$ in step 3. Hence, $\mathbf{t}^k_{q,h}$ satisfies

the first-order condition for the $\mathbf{t}$-subproblem exactly. Thus, it is enough to check the residual of the first-order condition of the $\mathbf{s}$-subproblem in the discrete analogue of $H^{-1}(\Omega)$. As before, we compute

$$\mathbf{R}_{q,h}^k := -\nabla_h \left(\mathrm{div}_h \mathbf{s}_{q,h}^k + f\right) + q\left(\mathbf{s}_{q,h}^k - \mathbf{t}_{q,h}^k\right) + \boldsymbol{\mu}_{q,h}^k, \tag{3.24}$$

find the solution of $-\Delta_h \tilde{\mathbf{R}}_{q,h}^k = \mathbf{R}_{q,h}^k$ with homogeneous Dirichlet boundary conditions on $\partial\Omega$ and otherwise proceed as in the previous subsection with some prescribed $\epsilon_d > 0$ for the termination condition (3.19).

Utilizing duality, an approximate solution to the discrete TV-problem is given by

$$u_{q,h}^* = \mathrm{div}_h \mathbf{s}_{q,h}^* + f. \tag{3.25}$$

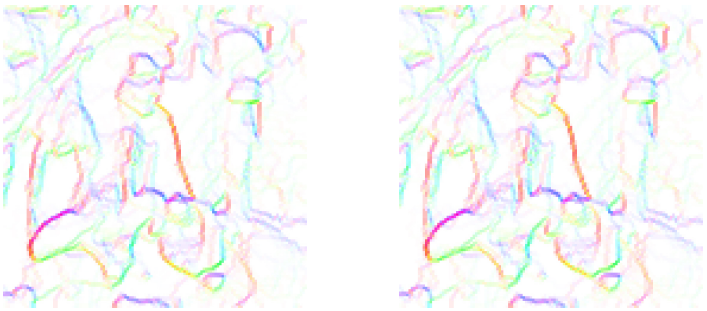

(a) (b)

Fig. 3.2: Figures (a) and (b) show the HSV-color-map, with $V = 1$, for the vector fields $\boldsymbol{\mu}^*$ and $\nabla_h u^*$, respectively, as obtained by Algorithm 4.

Suppose $\{(\mathbf{s}_{q,h}^k, \mathbf{t}_{q,h}^k, \boldsymbol{\mu}_{q,h}^k)\}_{k\in\mathbb{N}}$ is a sequence generated by Algorithm 4 and that it converges to $(\mathbf{s}^*, \mathbf{t}^*, \boldsymbol{\mu}^*) := (\mathbf{s}_{q,h}^*, \mathbf{t}_{q,h}^*, \boldsymbol{\mu}_{q,h}^*)$ with a fixed $q > 0$ and $h$. Then the first-order optimality conditions associated with the steps of Algorithm 4 are given by

$$-\nabla_h(\mathrm{div}_h \mathbf{s}^* + f) + q(\mathbf{s}^* - \mathbf{t}^*) + \boldsymbol{\mu}^* = \mathbf{0}, \tag{3.26a}$$

$$\max\left\{\alpha, \left|\frac{\boldsymbol{\mu}^*}{q} + \mathbf{s}^*\right|\right\}\mathbf{t}^* = \alpha\left(\frac{\boldsymbol{\mu}^*}{q} + \mathbf{s}^*\right), \tag{3.26b}$$

$$\mathbf{t}^* = \mathbf{s}^*. \tag{3.26c}$$

Since $u^* = \mathrm{div}_h \mathbf{s}^* + f$, we have

$$\boldsymbol{\mu}^* = \nabla_h u^*, \tag{3.27}$$

and further

$$\max\left\{\alpha, \left|\mathbf{s}^* + \frac{\nabla_h u^*}{q}\right|\right\}\mathbf{s}^* = \alpha\left(\mathbf{s}^* + \frac{\nabla_h u^*}{q}\right). \tag{3.28}$$

It can be shown that $u^*$ and $\mathbf{s}^*$ satisfy the first-order optimality conditions (in finite dimensions) associated with the (pre-)dual formulation of the TV-problem (2.1). In the left plot of Figure 3.2 we depict the numerical solution $\boldsymbol{\mu}^*$, which was obtained with a very large penalty parameter ($q = 2^{25}$) and the same continuation techniques as described in subsection 3.2.1. The regularization parameter was $\alpha = 0.2$, $\epsilon_d = 10^{-6}$ and we used the example in Figure 3.1(a). For the visualization we utilize an HSV-color space with $V = 1$ to represent the vector fields of $\boldsymbol{\mu}^*$ and $\nabla_h u^* = \nabla_h(\mathrm{div}_h \mathbf{s}^* + f)$ in Figure 3.2(a) and Figure 3.2(b), respectively. This color map allows to represent vectors in an RGB color model, i.e., matching colors between the two plots correspond to matching vector orientations. From these plots we observe that $\boldsymbol{\mu}^*$ obtained from Algorithm 4 numerically converges indeed to $\nabla_h u^*$.

Unlike the penalty method in subsection 3.2.1, the proposed algorithm in (4) obtains a numerical solution of (3.1) without the need of driving the penalty parameter to infinity. Moreover, we numerically observe that, with the same penalty parameter, Algorithm 4 achieves the stopping condition $|\nabla_h \tilde{\mathbf{R}}^k_{n,h}|_{\mathbf{L}^2} \leq \epsilon_d$ earlier than Algorithm 3.

**4. Staggered grid and numerical results.** In this section, we provide details of the discretization scheme (on a staggered grid) and analyze the numerical solvers of the subproblems in the minimization of (3.5) and (3.13). Moreover, we include evidence of the advantages of using a staggered grid to solve the proposed systems and we compare with results obtained by other algorithms.

Considering the finite element method, Raviart-Thomas elements on a rectangular mesh are an appropriate choice for discretizing the spaces considered while minimizing the proposed functionals in (3.5) and (3.13); see [10] for a specification of the Raviart-Thomas finite element space. This is due to the resulting discrete space being a finite dimensional subspace of $H_0(\mathrm{div})$. In the case of the finite difference method, we propose to use standard finite difference operators on a staggered grid. This is inspired by the fact that the lowest order Raviart-Thomas space on a rectangular mesh is equivalent to the "marker and cell" scheme (see [13]) which is a stable finite difference scheme for incompressible flow problems (see [17]).

**4.1. Finite difference operators on a staggered grid.** We consider the domain $\Omega = (0,1) \times (0,1)$ and the mesh size $h = 1/N$ for a positive integer $N \geq 2$. Figure 4.1(a) depicts an example for a grid associated with a $4 \times 4$ pixel image, i.e., $N = 4$. The outermost boundary is the boundary of the image $\partial\Omega$. For the subsequent discretization of the involved operators we define the index sets

$$\begin{aligned}
\Omega_h^{(a,b)} &:= \{(i,j) \in \mathbb{N} \times \mathbb{N} \mid 1 \leq i \leq N - a,\ 1 \leq j \leq N - b\}, \\
&\qquad \text{with} \quad (a,b) \in \{(1,0),\ (0,0),\ (0,1)\}, \\
\bar{\Omega}_h^{(0,0)} &:= \Omega_h^{(0,0)} \cup \{(i,0) \text{ or } (i,N+1) \mid 1 \leq i \leq N\} \cup \{(0,j) \text{ or } (N+1,j) \mid 1 \leq j \leq N\}, \\
\bar{\Omega}_h^{(1,0)} &:= \Omega_h^{(1,0)} \cup \{(0,j) \text{ or } (N,j) \mid 1 \leq j \leq N\}, \\
\bar{\Omega}_h^{(0,1)} &:= \Omega_h^{(0,1)} \cup \{(i,0) \text{ or } (i,N) \mid 1 \leq i \leq N\}.
\end{aligned}$$

The sets $\Omega_h^{(0,0)}$, $\Omega_h^{(1,0)}$ and $\Omega_h^{(0,1)}$ are identified with the set of $\bullet$-nodes, $\circ$-nodes, and $\square$-nodes in Figure 4.1, respectively. The set $\bar{\Omega}_h^{(0,0)}$ is identified with the $\bullet$-nodes

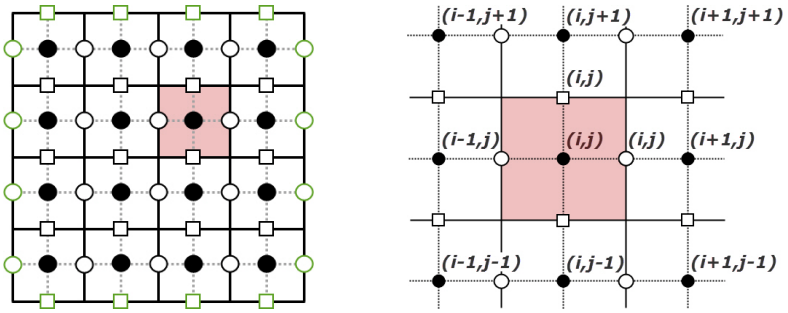


(a) (b)

Fig. 4.1: An example of a staggered grid for an image of size is $4 \times 4$. In (a) we depict $\Omega = (0,1) \times (0,1)$ with a discrete grid of mesh size $h = 1/4$. Note that the Green nodes are exactly placed on the boundary $\partial\Omega$ of the domain $\Omega$. In (b) a rule of indexing for different variables in (3.5) and (3.12) is depicted.

together with all the boundary nodes, $\bar{\Omega}_h^{(1,0)}$ with the $\circ$-nodes in addition to the nodes on the vertical boundary and $\bar{\Omega}_h^{(0,1)}$ with the $\square$-nodes and the nodes on the horizontal boundary, again depicted in Figure 4.1.

We define sets of real-valued functions on a discrete domain by

$$\mathcal{F}(\Omega_h^{(a,b)}) := \{f | f : \Omega_h^{(a,b)} \to \mathbb{R}\}. \tag{4.1}$$

Since the mesh size $h$ is fixed, we simply write

$$\mathcal{F}^{(a,b)} := \mathcal{F}(\Omega_h^{(a,b)}) \quad \text{and} \quad \bar{\mathcal{F}}^{(a,b)} := \mathcal{F}(\bar{\Omega}_h^{(a,b)}). \tag{4.2}$$

Note that following the identification of the sets $\Omega_h^{(a,b)}$ and $\bar{\Omega}_h^{(a,b)}$ with their corresponding nodes, we identify $\mathcal{F}^{(0,0)}$, $\mathcal{F}^{(1,0)}$, and $\mathcal{F}^{(0,1)}$ with the set of real-valued functions defined on the $\bullet$-nodes, the $\circ$-nodes, and the $\square$-nodes, respectively. Similar and analogous identifications are considered on the $\bar{\mathcal{F}}^{(a,b)}$ sets.

Now, we define two finite difference operators on a staggered grid: the discrete divergence

$$\mathrm{div}_h : \bar{\mathcal{F}}^{(1,0)} \times \bar{\mathcal{F}}^{(0,1)} \to \mathcal{F}^{(0,0)} \quad \text{by} \quad \mathrm{div}_h \mathbf{s} := \partial_1^- s_1 + \partial_2^- s_2 \in \mathcal{F}^{(0,0)}, \tag{4.3}$$

and the discrete gradient

$$\nabla_h : \mathcal{F}^{(0,0)} \to \mathcal{F}^{(1,0)} \times \mathcal{F}^{(0,1)} \quad \text{by} \quad \nabla_h u := (\partial_1^+ u, \partial_2^+ u) \in \mathcal{F}^{(1,0)} \times \mathcal{F}^{(0,1)}. \tag{4.4}$$

The standard finite forward and backward difference operators are defined by

$$(\partial_1^\pm f)_{i,j} = \pm \frac{f_{i\pm1,j} - f_{i,j}}{h} \quad \text{and} \quad (\partial_2^\pm f)_{i,j} = \pm \frac{f_{i,j\pm1} - f_{i,j}}{h}. \tag{4.5}$$

We also denote standard finite central difference operators by

$$(\partial_1 f)_{i,j} = \frac{f_{i+1,j} - f_{i-1,j}}{2h} \quad \text{and} \quad (\partial_2 f)_{i,j} = \frac{f_{i,j+1} - f_{i,j-1}}{2h}. \tag{4.6}$$

Even though the discrete divergence $\mathrm{div}_h$ and gradient $\nabla_h$ are defined by standard finite forward and backward operators, they can be interpreted as a central difference scheme because of the structure of the node distribution on the staggered grid.

**4.2. Compatibility of adjoint operators and boundary condition.** We recall that the solution space of the Fenchel pre-dual problem (3.1) is $H_0(\mathrm{div})$. On a staggered grid the discretize version of $H_0(\mathrm{div})$ becomes

$$H_0^{\mathcal{F}}(\mathrm{div}) := \left\{ (s_1, s_2) \in \bar{\mathcal{F}}^{(1,0)} \times \bar{\mathcal{F}}^{(0,1)} \;\middle|\; \begin{array}{l} (s_1)_{i,j} = 0,\ (i,j) \in \bar{\Omega}_h^{(1,0)} \setminus \Omega_h^{(1,0)}, \\ (s_2)_{i,j} = 0,\ (i,j) \in \bar{\Omega}_h^{(0,1)} \setminus \Omega_h^{(0,1)} \end{array} \right\}.$$

For this space, it can be shown that the discrete divergence (4.3) and gradient (4.4) are adjoint to each other under appropriate conditions. Indeed, for $\mathbf{s} \in H_0^{\mathcal{F}}(\mathrm{div})$ and $u \in \mathcal{F}^{(0,0)}$ we have

$$\begin{aligned} \langle u, -\mathrm{div}_h \mathbf{s} \rangle_{\mathcal{F}^{(0,0)}} &= \sum_{(i,j) \in \Omega_h^{(0,0)}} u_{i,j} (-\mathrm{div}_h \mathbf{s})_{i,j} \\ &= \sum_{(i,j) \in \Omega_h^{(1,0)}} (s_1)_{i,j} (\partial_1^+ u)_{i,j} + \sum_{(i,j) \in \Omega_h^{(0,1)}} (s_2)_{i,j} (\partial_2^+ u)_{i,j} \\ &= \langle \mathbf{s}, \nabla_h u \rangle_{\mathcal{F}^{(1,0)} \times \mathcal{F}^{(0,1)}}, \end{aligned} \tag{4.7}$$

where in the last line we consider $\mathbf{s}$ restricted to $\Omega_h^{(1,0)} \times \Omega_h^{(0,1)}$. Note that (4.7) might not hold for arbitrary $\mathbf{s} \in \bar{\mathcal{F}}^{(1,0)} \times \bar{\mathcal{F}}^{(0,1)} \setminus H_0^{\mathcal{F}}(\mathrm{div})$.

The discrete divergence and gradient oprerators introduced by Chambolle in [5] are formally of the same form as the ones in (4.3) and (4.4), respectively. However, it should be noted that for the discrete operators in [5], evaluations for all variables are computed on the same nodes. Hence, in order to obtain that the discrete gradient is the adjoint of the negative discrete divergence, additional boundary conditions for the primal variable are required.

**4.3. Numerical algorithms.** We now provide details on the numerical implementation of Algorithm2 on a staggered grid (the extension of the method for the minimization of (3.12) is straightforward). Note that the discrete functionals in (3.16) and (3.23) are typical discretizations of (3.5) and (3.12), respectively, when all variables are evaluated on the $\bullet$-nodes; see Figure 4.1.

The variables $\bar{u}, f, \mathbf{s}, \mathbf{t}$ and $\boldsymbol{\lambda}$ in (3.2), (3.16) and (3.23) associated to discrete spaces are as follows:

$$\bar{u},\ f \in \mathcal{F}^{(0,0)}, \quad \mathbf{s} \in H_0^{\mathcal{F}}(\mathrm{div}), \quad \mathbf{t},\ \boldsymbol{\lambda} \in \mathcal{F}^{(1,0)} \times \mathcal{F}^{(0,1)}. \tag{4.8}$$

Since the first and second components of a vector field on a staggered grid are evaluated at different locations, we need an interpolation operator whenever a function value is needed at an alternative location. Here, we use a simple linear interpolation. In fact, for given $\mathbf{s} \in \mathcal{F}^{(1,0)} \times \mathcal{F}^{(0,1)}$, the following averaging operators are used:

$$\mathcal{A}(s_2)_{i,j} = \frac{(s_2)_{i,j} + (s_2)_{i+1,j} + (s_2)_{i,j-1} + (s_2)_{i+1,j-1}}{4}, \quad \text{for } (i,j) \in \Omega_h^{(1,0)},\ s_2 \in \bar{\mathcal{F}}^{(0,1)}, \tag{4.9}$$

$$\mathcal{A}(s_1)_{i,j} = \frac{(s_1)_{i,j} + (s_1)_{i,j+1} + (s_1)_{i-1,j} + (s_1)_{i-1,j+1}}{4}, \quad \text{for } (i,j) \in \Omega_h^{(0,1)},\ s_1 \in \bar{\mathcal{F}}^{(1,0)}. \tag{4.10}$$

Consequently and depending on the nodes, the absolute values of $\mathbf{s} \in \mathcal{F}^{(1,0)} \times \mathcal{F}^{(0,1)}$

are defined by

$$|\mathbf{s}_{i,j}|^2 = (s_1)_{i,j}^2 + \mathcal{A}(s_2)_{i,j}^2, \quad \text{for } (i,j) \in \Omega_h^{(1,0)}, \tag{4.11}$$

$$|\mathbf{s}_{i,j}|^2 = \mathcal{A}(s_1)_{i,j}^2 + (s_2)_{i,j}^2, \quad \text{for } (i,j) \in \Omega_h^{(0,1)}, \tag{4.12}$$

$$|\mathbf{s}_{i,j}|^2 = \left(\frac{(s_1)_{i,j} + (s_1)_{i-1,j}}{2}\right)^2 + \left(\frac{(s_2)_{i,j} + (s_2)_{i,j-1}}{2}\right)^2, \text{ for } (i,j) \in \Omega_h^{(0,0)}. \tag{4.13}$$

It should be noted that the above definitions are consistent as the mesh size tends to zero under a continuity assumption: In fact, for $(i,j) \in \Omega_h^{(a,b)}$ with $(a,b) \in \{(1,0),\ (0,0),\ (0,1)\}$ let $s_1, s_2 \in C(\bar{\Omega};\mathbb{R})$ and $(s_k)_{i,j}$ correspond to the pointwise evaluation of $s_k$ on the corresponding node. Then the relations (4.11)-(4.13) hold as $h \downarrow 0$. This yields the desired inequality $|\mathbf{s}(\mathbf{x})| \leq \alpha$ for all $\mathbf{x} \in \Omega$.

Suppose $q_n > 0$ and $0 < \eta < 1$ are fixed and $\mathbf{t}_\eta^0$ is given. Denote by $\{(\mathbf{s}_n^k, \mathbf{t}_n^k)\}_{k\in\mathbb{N}}$ the sequence generated by Algorithm 2. According to first-order optimality, $\mathbf{s}_n^k$ solves the system

$$\begin{aligned} -\nabla(\mathrm{div}\mathbf{s} + f) + q_n(\mathbf{s} - \eta\mathbf{t}_n^{k-1}) &= \mathbf{0} \quad \text{in } \Omega, \\ \mathbf{s}\cdot\nu &= 0 \quad \text{on } \partial\Omega, \end{aligned} \tag{4.14}$$

and $\mathbf{t}_n^k$ is obtained in closed form by

$$\mathbf{t}_n^k(\mathbf{x}) = \begin{cases} \mathbf{s}_n^k(\mathbf{x}), & \text{if } |\mathbf{s}_n^k(\mathbf{x})| > \alpha,\ \mathbf{x} \in \Omega, \\ \frac{\mathbf{s}_n^k(\mathbf{x})}{|\mathbf{s}_n^k(\mathbf{x})|}, & \text{if } |\mathbf{s}_n^k(\mathbf{x})| \leq \alpha,\ \mathbf{x} \in \Omega. \end{cases} \tag{4.15}$$

Considering the staggered grid in Figure 4.1, we solve the two subproblems in Algorithm 2 by using the discrete operators (4.3) and (4.4). For a fixed mesh size $h$, the solution $\mathbf{s}_{n,h}^k \in H_0^{\mathcal{F}}(\mathrm{div})$ of the discrete $\mathbf{s}$-subproblem is obtained by solving

$$\begin{aligned} -\partial_1^+((\partial_1^- s_1)_{i,j} + (\partial_2^- s_2)_{i,j}) + q_n(s_1)_{i,j} &= (\partial_1^+ f)_{i,j} + q_n\eta((t_1)_{n,h}^{k-1})_{i,j}, \quad (i,j) \in \Omega_h^{(1,0)}, \\ -\partial_2^+((\partial_1^- s_1)_{i,j} + (\partial_2^- s_2)_{i,j}) + q_n(s_2)_{i,j} &= (\partial_2^+ f)_{i,j} + q_n\eta((t_2)_{n,h}^{k-1})_{i,j}, \quad (i,j) \in \Omega_h^{(0,1)}, \\ (s_1)_{i,j} &= 0, \quad (i,j) \in \bar{\Omega}_h^{(1,0)} \setminus \Omega_h^{(1,0)}, \\ (s_2)_{i,j} &= 0, \quad (i,j) \in \bar{\Omega}_h^{(0,1)} \setminus \Omega_h^{(0,1)}. \end{aligned} \tag{4.16}$$

Further, $\mathbf{t}_{n,h}^k \in \mathcal{F}^{(1,0)} \times \mathcal{F}^{(0,1)}$ is computed as

$$\begin{aligned} ((t_1)_{n,h}^k)_{i,j} &= \begin{cases} ((s_1)_{n,h}^k)_{i,j}, & \text{if } |\mathbf{s}_{n,h}^k|_{i,j} > \alpha,\ (i,j) \in \Omega_h^{(1,0)}, \\ \frac{((s_1)_n^k)_{i,j}}{|\mathbf{s}_{n,h}^k|_{i,j}}, & \text{if } |\mathbf{s}_{n,h}^k|_{i,j} \leq \alpha,\ (i,j) \in \Omega_h^{(1,0)}, \end{cases} \\ ((t_2)_{n,h}^k)_{i,j} &= \begin{cases} ((s_2)_{n,h}^k)_{i,j}, & \text{if } |\mathbf{s}_{n,h}^k|_{i,j} > \alpha,\ (i,j) \in \Omega_h^{(0,1)}, \\ \frac{((s_2)_{n,h}^k)_{i,j}}{|\mathbf{s}_{n,h}^k|_{i,j}}, & \text{if } |\mathbf{s}_{n,h}^k|_{i,j} \leq \alpha,\ (i,j) \in \Omega_h^{(0,1)}. \end{cases} \end{aligned} \tag{4.17}$$

As the solution in $\mathbf{t}$ is exact, the iteration along $k$ is stopped when the discrete residual of the optimality condition for the $\mathbf{s}$-subproblem is sufficiently small. In fact, since the equation in the first line of (4.14) holds in $H^{-1}(\Omega)$, a special step is require to measure the residual. For this purpose, after we extend $\mathbf{t}_{n,h}^k \in \mathcal{F}^{(1,0)} \times \mathcal{F}^{(0,1)}$

to $H_0^{\mathcal{F}}(\mathrm{div})$ and $f \in \mathcal{F}^{(0,0)}$ to $\bar{\mathcal{F}}^{(0,0)}$ by homogeneous Neumann boundary conditions on $\partial\Omega$, we compute the vector field

$$\mathbf{R}_{n,h}^k := -\nabla_h \left(\mathrm{div}_h \mathbf{s}_{n,h}^k + f\right) + q_n \left(\mathbf{s}_{n,h}^k - \eta \mathbf{t}_{n,h}^k\right) \in \bar{\mathcal{F}}^{(1,0)} \times \bar{\mathcal{F}}^{(0,1)}, \tag{4.18}$$

and find $\tilde{\mathbf{R}}_{n,h}^k = ((\tilde{R}_1)_{n,h}^k, (\tilde{R}_2)_{n,h}^k) \in \bar{\mathcal{F}}^{(0,0)} \times \bar{\mathcal{F}}^{(0,0)}$ as the solution of

$$-((\partial_1^+\partial_1^- + \partial_2^+\partial_2^-)(\tilde{R}_l)_{n,h}^k)_{i,j} = \frac{1}{2}\left(((R_l)_{n,h}^k)_{i,j} + ((R_l)_{n,h}^k)_{i-(2-l),j-(l-1)}\right), \quad (i,j) \in \Omega_h^{(0,0)}, \tag{4.19}$$

$$((\tilde{R}_l)_{n,h}^k)_{i,j} = 0, \quad (i,j) \in \bar{\Omega}_h^{(0,0)} \setminus \Omega_h^{(0,0)}, \tag{4.20}$$

for $l \in \{1,2\}$. The numerical solution, $\mathbf{s}_{n,h}^* := \mathbf{s}_{n,h}^k$, is obtained for the smallest $k \geq 1$ such that

$$|\nabla_h \tilde{\mathbf{R}}_{n,h}^k|_{\mathbf{L}^2} \approx \left( h^2 \sum_{\substack{l\in\{1,2\} \\ (i,j)\in\Omega_h^{(0,0)}}} |(\partial_1(\tilde{R}_l)_{n,h}^k)_{i,j}|^2 + |(\partial_2(\tilde{R}_l)_{n,h}^k)_{i,j}|^2 \right)^{\frac{1}{2}} \leq \epsilon_d, \tag{4.21}$$

for a prescribed stopping tolerance $\epsilon_d > 0$.

The approximate solution of the discrete TV-problem is then given by

$$(u_{n,h}^*)_{i,j} = (\mathrm{div}_h \mathbf{s}_{n,h}^*)_{i,j} + f_{i,j}, \quad (i,j) \in \Omega_h^{(0,0)}. \tag{4.22}$$

For increasing $q_n$, we use the same continuation scheme as described before.

**4.4. Additional Numerical Results.** Next we compare our results numerically with those obtained from different algorithms. In all examples below the respective image intensity is scaled to $[0,1]$. For simplicity we use the following abbreviations for the methods of Sections 2 and 3:

- $P_{ALM}$ : Primal augmented Lagrangian method of subsection 2.1.1.
- $D_{ALM}$ : The augmented Lagrangian method of the Fenchel pre-dual formulation in subsection 3.2.2.

Note that we use the same discretization as in [27] for $P_{ALM}$. Unless otherwise specified, we use the previously described discretization on the staggered grid of subsection 4.1 for $D_{ALM}$.

First, we provide a qualitative comparison between $P_{ALM}$ and $D_{ALM}$ in Figure 4.2. In order to ensure a fair comparison, we choose an example with

$$f = \chi_{\mathcal{C}}, \quad \mathcal{C} := \{\mathbf{x} \in (0,1)\times(0,1) \,:\, |\mathbf{x} - (0.5, 0.5)| \leq 0.3\}, \tag{4.23}$$

with known exact solution; see [23] or [24]. Figure 4.2(a) shows the $128 \times 128$ image $f$ in the TV-model. For $P_{ALM}$, $\epsilon_p = 10^{-2}$, $r_0 = 2^{-10}$ and $r_{n+1} = 2r_n$ are used. Figure 4.2(b) displays the numerical solution obtained by $P_{ALM}$ with penalty parameter $r_{22} = 2^{12}$. For $D_{ALM}$, $\epsilon_d = 10^{-6}$, $q_0 = 2^{10}$ and $q_{n+1} = 2q_n$ are used. Figure 4.2(c) shows the numerical solution obtained by $D_{ALM}$ with penalty parameter $q_{15} = 2^{25}$. We use the same idea as proposed in [6] to change a gray-scale image into a color image based on the color table in Figure 4.2(d). Figure 4.2(e) and Figure 4.2(f) are the color images corresponding to Figure 4.2(b) and Figure 4.2(c), respectively, based on the aforementioned color table.

We readily observe that the results of $P_{ALM}$ in Figures 4.2(b) and 4.2(e) suffer from blurriness depending on radial directions from the center of the circle. The direction dependent error is caused by the one-sided discretization scheme in [27]. It is significantly reduced by using the upwind finite-difference method in [6]. The errors responsible for blurry regions in the reconstruction cannot be overcome by the algorithms in Section 2 as the solution space in case of a finite penalty parameter is $W^{1,1}(\Omega)$. The latter does not admit edge structures. On the other hand, the Fenchel pre-dual formulation is crucially different in this respect. The numerical result from $D_{ALM}$ seems to approximate a piece-wise constant function with the exception of a small number of pixels (compare, for example, with the results obtained in [6, Figure 5.1]). We also note that the one-sided discretization scheme of [27] for the algorithms in Section 3 generate a result similar to Figure 4.2(b).

In Figure 4.3, the original image is degraded by Gaussian white noise with a standard deviation of 20. Figure 4.3(a) shows the $128 \times 128$ noisy image $f$ in the TV-model. A relatively large regularization parameter $\alpha = 1$ is used, as we primarily want to study discretization aspects. In this respect, recovering "too" many detailed features in Figure 4.3(c) would render the comparison of effects at boundaries between constant image features impossible. For $P_{ALM}$, $\epsilon_p = 10^{-2}$, $r_0 = 2^{-10}$ and $r_{n+1} = 2r_n$ are used. Figure 4.3(b) depicts the numerical solution obtained by $P_{ALM}$ when the penalty parameter is $r_{30} = 2^{20}$. For $D_{ALM}$, $\epsilon_d = 10^{-6}$, $q_0 = 2^{10}$ and $q_{n+1} = 2q_n$ are used. Figure 4.3(c) depicts the numerical solution obtained by $D_{ALM}$ when the penalty parameter reaches $q_{15} = 2^{25}$. Figures 4.3(d), 4.3(e), and 4.3(f) are the color images corresponding to 4.3(a), 4.3(b), and 4.3(c), respectively, based on the color table in Figure 4.2(d). We observe a similar behavior as in Figure 4.2. The numerical result from $D_{ALM}$ is piecewise constant which is supposed to be a solution of the TV-model, whereas the non-staggered grid is responsible for blurring effects at boundaries between contour pieces.

**5. Conclusion.** While variable splitting methods have been used successfully in image processing over the recent years, usually with the understanding that they solve a discrete version of, e.g., the TV-model, the situation for the original, genuinely infinite dimensional TV-model is different.

Primal variable splitting techniques are in general not well-defined as the existence of a solution of the associated penalty problem cannot be guaranteed. Rather it can be shown that for increasing penalty parameters, $\epsilon$-minimizers (in the sense of Ekeland's variational principle) converge to the solution of the TV-problem. Nevertheless, the alternating iteration schemes, often utilized for solving the penalty problem, appear functional, as the associated subproblems admit (unique) solutions. Their convergence, obviously, is jeopardized by the possible non-existence of solutions of the associated minimization problem.

The situation for the pre-dual problem (note that the dual would lead to a problem in the dual of the non-reflexive space of functions of bounded variation) is entirely different: (i) Variable splitting techniques are well-defined in the sense that associated penalty or augmented Lagrangian based problems admit solutions in function space; (ii) the pre-dual is posed in Hilbert space; and (iii) the associated alternating minimization, Bregman splitting or augmented Lagrangian methods exhibit guaranteed convergence properties and perform better than their primal counterparts (upon discretization).

Finally, as the pre-dual is posed in $H_0(\mathrm{div})$, staggered grids are appropriate for discretization as they provided stable (and numerically significantly less diffusive and

somewhat isotropic) finite difference schemes. In this paper this was validated numerically including a comparison with other specialized discretization schemes for dual formulations of the discrete TV-problem.

## REFERENCES


[1] R. A. Adams and J. J. F. Fournier. *Sobolev Spaces*. Academic Press, second edition, 2003.

[2] L. Ambrosio, N. Fusco, and D. Pallara. *Functions of Bounded Variation and Free Discontinuity Problems*. Oxford Mathematical Monographs, 2000.

[3] H. Attouch, G. Buttazzo, and G. Michaille. *Variational Analysis in Sobolev and BV Spaces*. MPS-SIAM, 2006.

[4] E. Casas, K. Kunisch, and C. Pola. Regularization by functions of bounded variation and applications to image enhancement. *Applied Mathematics and Optimization*, 40:229–257, 1999.

[5] A. Chambolle. An algorithm for total variational minimization and applications. *J. Math. Imaging Vis.*, 20:89–97, 2004.

[6] A. Chambolle, S.E. Levine, and B.J. Lucier. An upwind finite-difference method for total variation-based image smoothing. *SIAM J. Imaging Sci.*, 4:277–299, 2011.

[7] R. Chan, M. Tao, and X. Yuan. Constrained total variation deblurring models and fast algorithms based on alternating direction method of multipliers. *SIAM Journal on Imaging Sciences*, 6(1):680–697, 2013.

[8] K. Chen, Y. Dong, and M. Hintermüller. A nonlinear multigrid solver with line Gauss-Seidel-semismooth-Newton smoother for the Fenchel pre-dual in total variation based image restoration. *Inverse Problems and Imaging*, 5(2):323–339, 2011.

[9] Y. Chen, W. Hager, F. Huang, D. Phan, X. Ye, and W. Yin. Fast algorithms for image reconstruction with application to partially parallel mr imaging. *SIAM Journal on Imaging Sciences*, 5(1):90–118, 2012.

[10] A. Ern and J.L. Guermond. *Theory and Practice of Finite Elements*. Number v. 159 in Applied Mathematical Sciences. Springer, 2004.

[11] E. Giusti. *Minimal Surfaces and Functions of Bounded Variation*. Birkhäuser, 1984.

[12] T. Goldstein and S. Osher. The split Bregman method for L1-regularized problems. *SIAM J. Img. Sci.*, 2:323–343, 2009.

[13] F. H. Harlow and J. E. Welch. Numerical calculation of time-dependent viscous incompressible flow of fluid with free surface. *Phys. Fluids*, 8(12):2182–2189, 1965.

[14] M. Hintermüller and K. Kunisch. Total bounded variation regularization as a bilaterally constrained optimization problem. *SIAM Journal of Applied Mathematics*, 64:1311–1333, 2004.

[15] M. Hintermüller and G. Stadler. An infeasible primal-dual algorithm for total bounded variation-based inf-convolution-type image restoration. *SIAM Journal of Scientific Computing*, 28:1–23, 2006.

[16] K. Ito and K. Kunisch. An active set strategy based on the augmented Lagrangian formulation for image restoration. *ESAIM: Mathematical Modelling and Numerical Analysis*, 33:1–21, 1999.

[17] G. Kanschat. Divergence-free discontinuous Galerkin schemes for the Stokes equations and the MAC scheme. *Int. J. Numer. Methods Fluids*, 56(7):941–950, 2008.

[18] S. Kurcyusz. On the existence and nonexistence of Lagrange multipliers in banach spaces. *Journal of Optimization Theory and Applications*, 20(1):81–110, 1976.

[19] D. G. Luenberger. *Optimization by Vector Space Methods*. John Wiley & Sons, 1969.

[20] M. Ng, P. Weiss, and X. Yuan. Solving constrained total-variation image restoration and reconstruction problems via alternating direction methods. *SIAM Journal on Imaging Sciences*, 32(5):2710–2736, 2010.

[21] L. I. Rudin, S. Osher, and E. Fatemi. Nonlinear total variation based noise removal algorithms. *Physica D*, 60:259–268, 1992.

[22] S. Setzer. Operator splittings, Bregman methods and frame shrinkage in image processing. *Int. J. Comput. Vis*, 92(3):265–280, 2011.

[23] D. M. Strong and T. F. Chan. Exact solutions to total variation regularization problems. Technical report, UCLA CAM Report, 1996.

[24] D. M. Strong and T. F. Chan. Edge-preserving and scale-dependent properties of total variation regularization. *Inverse Problems*, 19:165–187, 2003.

[25] X.-C. Tai and C. Wu. Augmented Lagrangian method, dual methods and split Bregman iteration for ROF model. In *SSVM '09: Proceedings of the Second International Conference*

*on Scale Space and Variational Methods in Computer Vision*, pages 502–513, Berlin, Heidelberg, 2009. Springer-Verlag.

[26] Y. Wang, J. Yang, W. Yin, and Y. Zhang. A new alternating minimization algorithm for total variation image reconstruction. *SIAM Journal on Imaging Sciences*, 1:248–272, 2008.

[27] C. Wu and X.-C. Tai. Augmented Lagrangian method, dual methods, and split Bregman iteration for ROF, vectorial TV, and high order models. *SIAM Journal on Imaging Sciences*, 3(3):300–339, 2010.

[28] J. Yang, W. Yin, Y. Zhang, and Y. Wang. A fast algorithm for edge-preserving variational multichannel image restoration. *SIAM Journal on Imaging Sciences*, 2(2):569–592, 2009.

[29] J. Zowe and S. Kurcyusz. Regularity and stability for the mathematical programming problem in Banach spaces. *Applied Mathematics and Optimization*, 5:49–62, 1979.

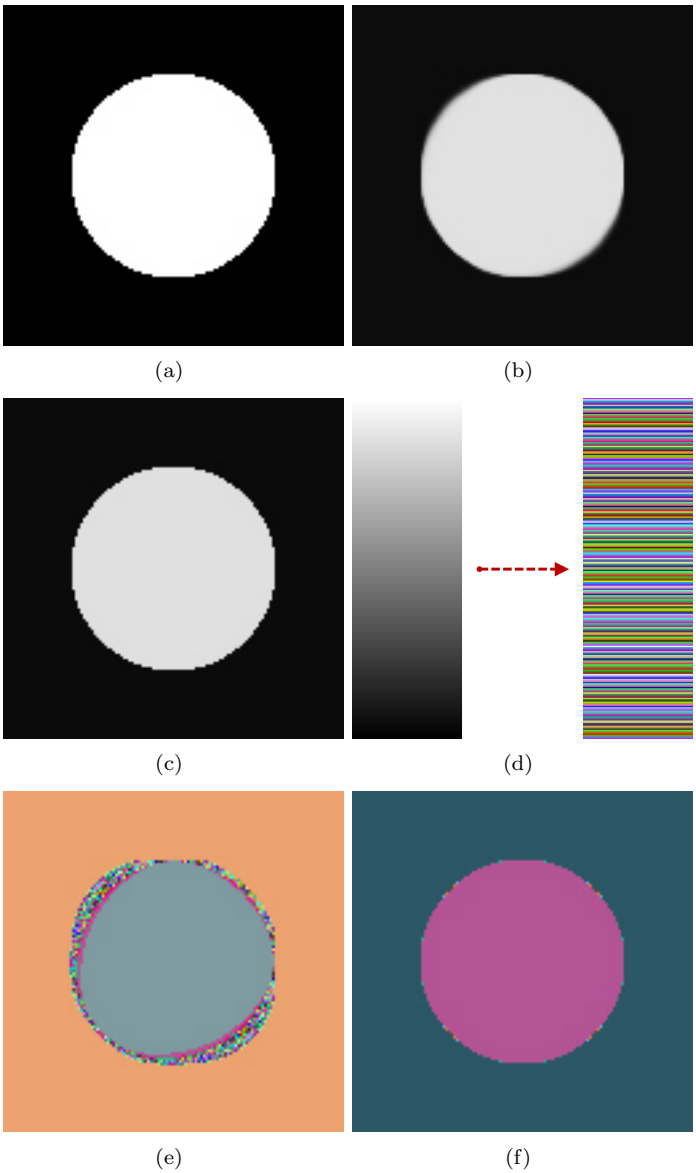

Fig. 4.2: A qualitative comparison between $P_{ALM}$ and $D_{ALM}$: (a) The $128 \times 128$ image $f$ for the TV-model. The results from $P_{ALM}$ and $D_{ALM}$ are shown in (b) and (c), respectively. The color table to change a gray-scale image into a color image is shown in (d). In (e) and (f), we show the correspondingly colored versions of the images in (b) and (c), respectively. It is easy to observe that $D_{ALM}$ generates an almost piecewise constant image.

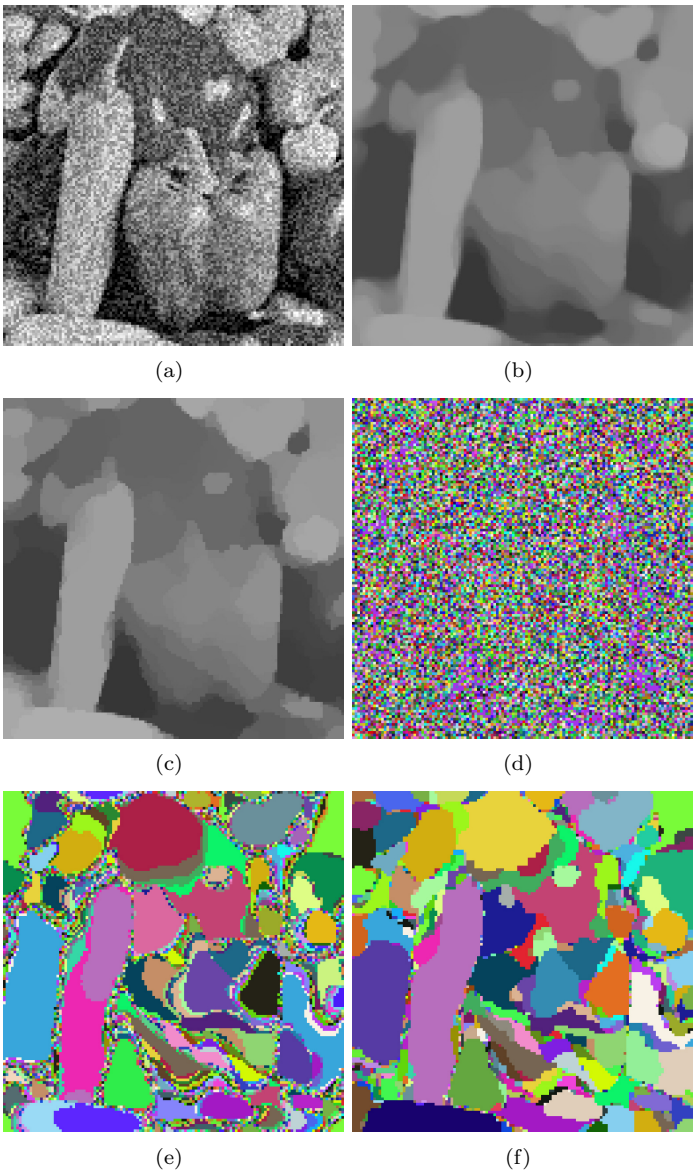

Fig. 4.3: A qualitative comparison between $P_{ALM}$ and $D_{ALM}$: (a) The $128 \times 128$ image $f$ in the TV-model. The results for $P_{ALM}$ and $D_{ALM}$ can be seen in (b) and (c), respectively. Figures (d), (e), and (f) are the corresponding color images to (a), (b) and (c), respectively, based on a color table in Figure 4.2(d).